

Chimia 46 (1992) 359–376  
 © Neue Schweizerische Chemische Gesellschaft  
 ISSN 0009–4293

# Photochemical and Photo-physical Studies within Zeolites

V. Ramamurthy\*

**Abstract.** In this article, we illustrate how one can utilize a zeolite matrix to control the photophysical and photochemical behavior of guest molecules included in them. In the first part, the emphasis is placed on the cation and on a single zeolite, faujasite (X and Y). Photophysical properties of naphthalene and other aromatic guest molecules included in X-type faujasite zeolites ( $M^+X$ ,  $M = \text{Li, Na, K, Rb, Cs, Tl}$ ) have been investigated. As expected for an external heavy-atom-perturbed excited state, both singlet- and triplet-excited-state lifetimes and emission efficiencies depend upon the identity and accessibility of the cation present within the zeolite supercage. The power of the heavy-atom-cation effect in zeolites has been demonstrated by recording phosphorescence from several olefins whose phosphorescence has not previously been recorded. The second section brings out an inherent feature of a field at its infancy-serendipity. Surprisingly, radical ions of organic molecules can be generated and stabilized within zeolites by a simple procedure. This study has been expanded to include oligomers of thiophenes and  $\alpha,\omega$ -diphenylpolyenes which serve as models for conducting polymers. This is followed by a presentation wherein the importance of the relative size of the host cavity to that of the guest to achieve maximum selectivity in a photoreaction is highlighted. Concepts developed in this section with faujasite and pentasil (ZSM-5 and ZSM-11) as models are believed to be general and applicable to other organized media.

## 1. Introduction

Organized media allow one to design a system and then carry out photochemical and photophysical studies within these assemblies in a more temporally and structurally quantifiable fashion than is possible in an isotropic media. In this context, organized media such as crystals, surfaces (silica, alumina, clay *etc.*), liquid crystals, micelles, mono- and bi-layers, inclusion complexes are being subjected to extensive investigation [1]. In the last few years, our as well as a few other groups' interest has turned to the use of zeolites as media for photoreactions [2]. In this presentation, a few of the observations made in our laboratory with zeolite as a medium for photoreactions are highlighted. For a general survey the readers are directed to recent reviews [2].

Zeolites may be regarded as open structures of silica in which aluminum has been substituted in a fraction of the tetrahedral sites [3]. The substitution of trivalent aluminum ions for a fraction of the tetravalent silicon ions at lattice positions results in a network that bears a net negative charge which must be compensated by other counter ions. As such, zeolites can be repre-

sented by the empirical formula  $M_{2/n} \cdot \text{Al}_2\text{O}_3 \cdot x \text{SiO}_2 \cdot y \text{H}_2\text{O}$ , where M is the cation of valence  $n$  (typically Na, Ca, Mg, *etc.*),  $x = 2 - \infty$ , and  $y$  varies from 0 to *ca.* 10. These cations can generally be exchanged by conventional methods. The latter are mobile and may occupy various exchange sites depending on their radius, charge, and degree of hydration. They can be



V. Ramamurthy was born near Madras, India. He obtained his M.Sc at Indian Institute of Technology, Madras, India (1968) and a Ph.D at University of Hawaii, USA (1974) under the direction of R.S.H. Liu. He carried out postdoctoral research at University of Western Ontario (1974–75) with P. de Mayo and at Columbia University (1975–78) with N.J. Turro. Following a stay on the faculty at Indian Institute of Science, Bangalore, India (1978–87), he joined the Central Research and Development Department of The Du Pont Company, Wilmington, USA, where he is at present. His contributions to photochemistry have been in the areas of thiocarbonyl photochemistry and photochemistry in organized media. This article is based on the address given on the occasion of the receipt of Grammaticakis-Neumann Prize for 1991.

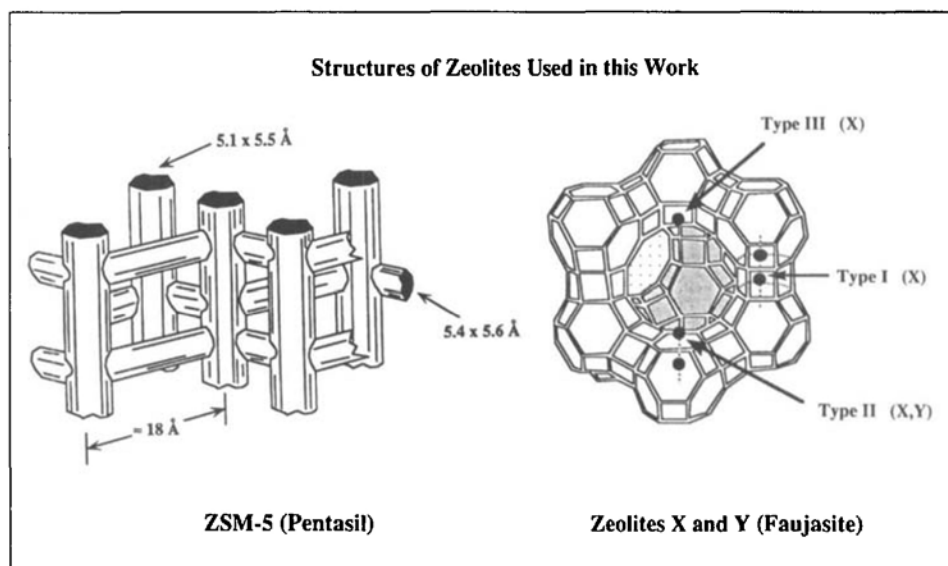


Fig. 1. Structures of zeolites: ZSM-5 and faujasites (X and Y). Position of cations in X and Y zeolites shown as type-I, -II, and -III [12].

\*Correspondence: Dr. V. Ramamurthy  
 Central Research and Development  
 Experimental Station  
 The Du Pont Company  
 Wilmington, Delaware 19880-0328, USA

Table 1. Size of Pore Openings and Dimensionality of the Pore System for Selected Medium-Pore and Large-Pore Molecular Sieves<sup>a)</sup>

Molecular Sieve Name	Pore (window) Size [Å]	Channel/Cage Size
Faujasite (X and Y type)	7.4	Three dimensional channel with a cage ( $d = 12 \text{ \AA}$ )
Omega	7.5 (3.4 x 5.6)	Two non-interconnected channels
Linde Type L	7.1	Single channel with a lobe ( $d \approx 7.5 \text{ \AA}$ )
Mordenite	7.0 x 6.7 and (2.6 x 5.7)	Two interconnected channels
Offretite	6.7 and (3.6 x 4.9)	Two interconnected channels
ZSM-34	6.7 and (3.6 x 4.9)	Two interconnected channels
ZSM-11	5.3 x 5.4	Two interconnected channels
ZSM-5	5.3 x 5.6 and 5.1 x 5.5	Two interconnected channels
Theta-1	4.4 x 5.5	Single channel
4A	4.2	Three dimensional channel with a cage ( $d = 12 \text{ \AA}$ )

<sup>a)</sup> W. M. Meier, D. H. Olson, in 'Atlas of Zeolite Structure Types', 2nd revised edn., Butterworths, Cambridge, 1987.  
D. W. Breck, 'Zeolite Molecular Sieves: Structure, Chemistry, and Use', John Wiley & Sons, New York, 1974.

Table 2. Photophysical Parameters for Naphthalene Included in Zeolites

Zeolite Host	Triplet Lifetime <sup>a)</sup> [s]	Singlet Lifetime <sup>b)</sup> [ns]	P/F <sup>c)</sup>
Li X	—	33.0	$1.0 \times 10^{-4}$
Na X	—	35.4	$7.3 \times 10^{-2}$
K X	1.72	19.4	0.16
Rb X	0.72	2.22	8.1
Cs X	0.20	0.23 (87%), 1.87 (13%)	45
Tl X	0.0012	—	only P
Li Y	—	31.8	$1.2 \times 10^{-3}$
Na Y	—	25.1	$1.0 \times 10^{-3}$
K Y	—	13.8	0.1
Rb Y	—	3.8	9.0
Cs Y	—	0.7	60

<sup>a)</sup> The lifetime measured at 77 K.

<sup>b)</sup> The lifetime measured at 298 K.

<sup>c)</sup> Phosphorescence to fluorescence intensity ratio estimated at 77 K; the number is independent of the wavelength of excitation.

replaced, to varying degrees, by exchange with other cations. The numerous framework topologies of the molecular sieves offer various systems of channels and cavities resulting in one-, two-, or three-dimensional diffusion for included guest molecules. There are two types of structures: one provides an internal pore system comprised of interconnected cage structures; the second provides a system of uniform channels. Access to these channels, cages, or cavities is through a pore or window which can be of the same size or smaller than the size of the channels, cages, or cavities. It is this pore dimension which determines the size of molecules that can be adsorbed into these structures.

The topological structure of X- and Y-type zeolites consists of an interconnected three-dimensional network of relatively large spherical cavities, termed supercages (diameter of *ca.* 13 Å; Fig. 1). Each supercage is connected tetrahedrally to four other supercages through 8-Å windows or pores. The interior of zeolites X and Y also contains, in addition to supercages, smaller sodalite cages. The windows to the sodalite cages are too small to allow organic molecules access to these cages. Charge compensating cations present in the internal structure are known to occupy three different positions in the zeolites X and Y (Fig. 1). Only cations of sites II and III are expected to be readily accessible to the adsorbed organic molecule.

Among the medium-pore sized zeolites, perhaps the most studied are the pentasil zeolites, ZSM-5 and ZSM-11 (Fig. 1). These zeolites also have three-dimensional pore structures; a major difference between the pentasil pore structures and the faujasites described above is the fact that the pentasil pores do not link cage structures as such. Instead, the pentasils are composed of two intersecting channel systems. For ZSM-5, one system consists of straight channels with a free diameter of *ca.* 5.4 x 5.6 Å and the other consists of sinusoidal channels with a free diameter of *ca.* 5.1 x 5.5 Å. For ZSM-11, both are straight channels with dimensions of *ca.* 5.3 x 5.4 Å. The volume at the intersections of these channels is estimated to be 370 Å<sup>3</sup> for a free diameter of about 8.9 Å. Other large-pore zeolites of interest for photochemical studies include the large-pore zeolites L, mordenite, offretite, omega, and beta, as well as the aluminophosphate frameworks AIPO<sub>4</sub>-5 (large-pore), AIPO<sub>4</sub>-8 (extra-large pore), and VPI-5 (very large-pore). Dimensions and cage/channel structures of various zeolites are provided in Table 1.

The presentation is divided into three main parts. In the first part, photophysical

aspects with an emphasis on heavy-atom effect are highlighted. In the second part, generation, stabilization, and study of radical ions within zeolites are discussed. In the last part, results of photochemical studies with 'reaction cavity' concept in mind are presented.

## 2. Variation in Spin-Orbit Coupling Parameter: Heavy-Atom (Cation) Effect [4]

In this section, we illustrate how the change in alkali cation present within supercages of faujasites alters the effective spin-orbit coupling available for a zeolite included guest molecule. Such changes offer an unique opportunity to control the distribution and decay of the singlet and the triplet excited states of guest molecules. By utilizing this technique, we have been able to observe phosphorescence for systems for which previous attempts to record phosphorescence have yielded only negative results.

### 2.1. Heavy-Atom (Cation) Effect within Zeolites-Phosphorescence from Aromatics

As shown in Fig. 2, the emission spectrum of naphthalene is profoundly affected by inclusion in faujasites [5]. For low-mass cations such as  $\text{Li}^+$  and  $\text{Na}^+$ , the emission spectra show the typical naphthalene blue fluorescence. However, as the mass of the cation increases (e.g., from  $\text{Rb}^+$  to  $\text{Cs}^+$  to  $\text{Tl}^+$ ), there is a dramatic decrease in fluorescence intensity and a simultaneous appearance of a new vibronically structured low-energy emission band that is readily identified as the phosphorescence of naphthalene. Table 2 lists excited singlet (at room temperature) and triplet lifetimes (at 77 K) of naphthalene included within various cation exchanged zeolites. It is clear that both these lifetimes are cation-dependent. On the basis of the following observations, we conclude that the heavy-cation effect is responsible for the enhanced phosphorescence and decreased singlet and triplet lifetimes for naphthalene within K, Rb, Cs, and Tl cation exchanged faujasites. It is well-known that the effect of external heavy-atom perturbation scales with the square of the perturber's spin-orbit coupling constant,  $\xi^2$  and that a log-log plot of  $\tau_T^{-1}$  vs.  $\xi^2$  should be linear with a maximum predicted slope of unity [6]. As shown in Fig. 3, the expected dependence is observed. For comparison, we have also provided in Fig. 3 the linear relationship observed in two systems, namely 1-halonaphthalenes [6] and 1,5-naphtho-22-crown-6 [7], where the external and internal heavy-atom ef-

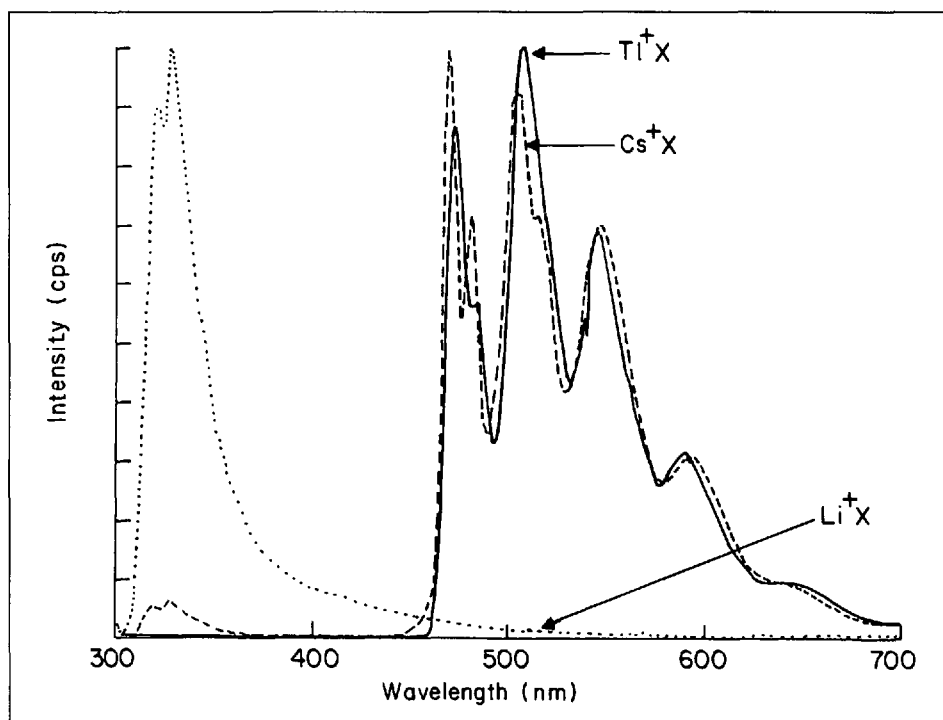


Fig. 2. Emission spectra at 77 K of naphthalene included in Li X, Cs X, and Tl X (excitation  $\lambda$ : 285 nm). Note the ratio of phosphorescence to fluorescence changes with the cation but the ratio change is independent of the excitation wavelength [12].

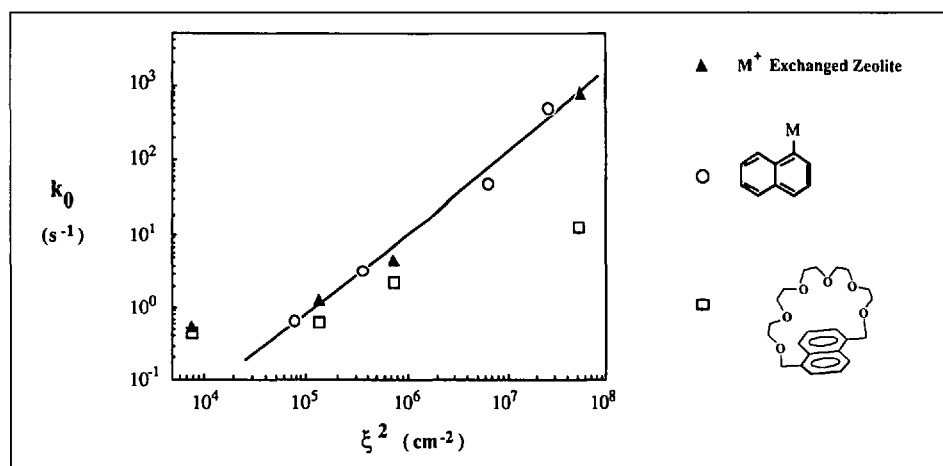


Fig. 3. A linear relationship between the triplet decay of naphthalene in M X zeolites and the spin-orbit coupling parameter of the cation. Similar relationships for 1-halonaphthalenes and cation complexed 1,5-naphtho-22-crown-6 are also shown [12][5].

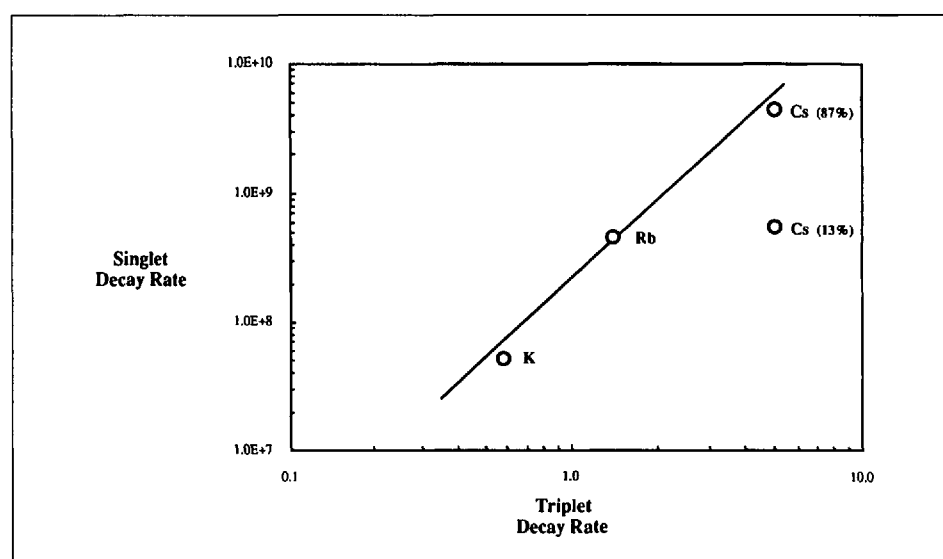


Fig. 4. Linear relationship between singlet and triplet decay of naphthalene in M X zeolites. Both singlet and triplet decays are influenced by the cation [12].

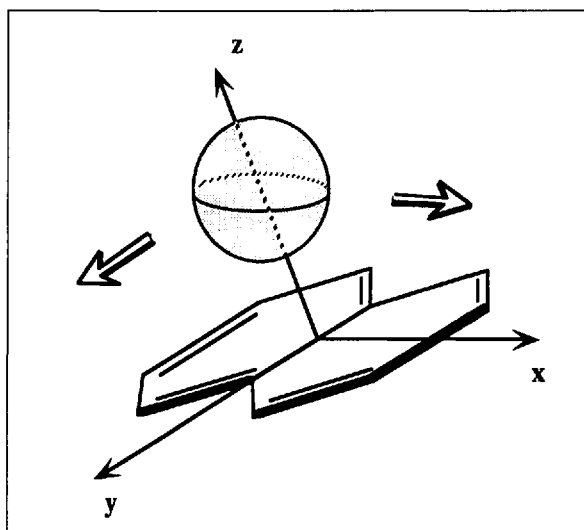


Fig. 5. Proposed geometry of interaction between naphthalene and cation within the supercage of faujasites

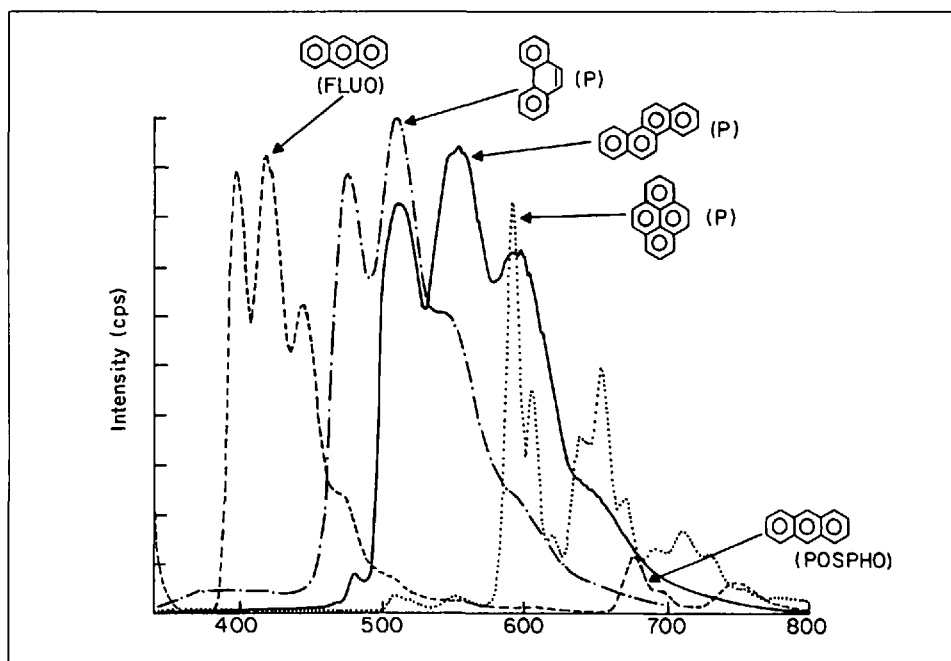


Fig. 6. Emission spectra at 298 K of anthracene (ex  $\lambda = 340$  nm), phenanthrene (ex  $\lambda = 295$  nm), chrysene (ex  $\lambda = 320$  nm), and pyrene (ex  $\lambda = 340$  nm) included in TlX. No fluorescence is seen in phenanthrene, chrysene, and pyrene under these conditions [12].

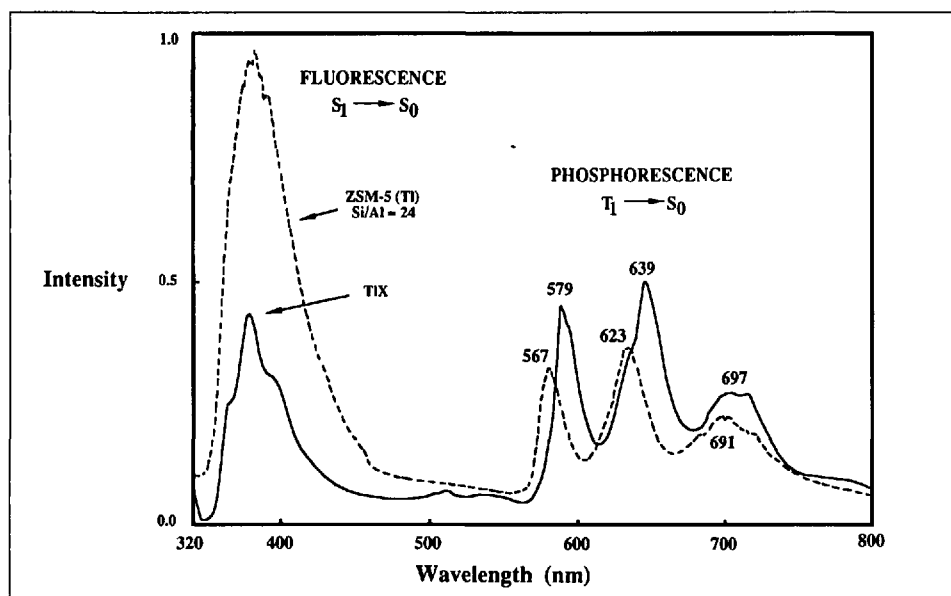


Fig. 7. Emission spectra at 298 K of (E)-stilbene included in TlX and in Tl ZSM-5 (excitation  $\lambda = 290$  nm; corning glass filter 0-51 is used to cut off the second order). Note the intense phosphorescence in both cases [10].

facts, respectively, are presumed to operate. The magnitude of the heavy-atom effect observed in zeolites is significantly larger than that observed for the 1,5-naphtho-22-crown-6 exchanged with heavy-atom cations where the cation is rigidly held over the naphthalene  $\pi$  face. In fact, the zeolite samples show heavy-atom effects nearly as large as for a series of 1-halonaphthalenes where the perturbers are covalently attached to the chromophore. This is attributable both to the close approach between naphthalene and the heavy atom which is enforced by the zeolite supercage and to the presence of more than one heavy-atom cation per supercage which leads to highly effective concentrations of the heavy-atom cation in the vicinity of the naphthalene molecule. If the heavy-cation effect is indeed responsible for the variations in singlet and triplet lifetimes, one would expect a linear relationship between singlet and triplet decays with cation variation. Indeed this is observed as shown in Fig. 4. The slope of the line suggests that the singlet decay is enhanced more than the triplet, consistent with the smaller energy gap between the  $S_1$  and  $T_1$  as compared to the  $T_1$  and  $S_0$ .

To obtain a picture of the geometry of the cation-aromatic (naphthalene) interaction in X- and Y-type faujasites, we took advantage of the heavy-atom-induced phosphorescence which allows the use of optical detection of magnetic resonance (ODMR) in zero applied magnetic field [8]. The sublevel specific dynamics for adsorbed naphthalene show a distinct increase in relative radiative character and total rate constant of the out-of-plane  $x$  sublevel with increasing mass of the cation perturber. Enhancement from only triplet sublevel  $T_x$  is expected for a heavy-atom approach along the  $x$  axis [9]. ODMR kinetic results suggests that the naphthalene is adsorbed through its  $\pi$  cloud at a cation site (Fig. 5).

The above heavy-cation effect within zeolites is found to be general. Enhanced phosphorescence is observed for a wide range of different organic guests such as anthracene, acenaphthene, phenanthrene, chrysene, fluoranthene, pyrene, and 1,2,3,6,7,8-hexahydropyrene when included in  $Tl^+$ -exchanged faujasites (Fig. 6). The only set of examples of guests for which phosphorescence is not observed are fused aromatics, which are too large in diameter to fit through the 8-Å windows of the X- and Y-type zeolites (e.g., coronene and triphenylene). Also this phenomenon is not restricted to faujasites alone. Enhanced phosphorescence has been observed for guest molecules within heavy-cation-exchanged ZSM-5, L, M-5,  $\Omega$ -5, and beta.

2.2. Phosphorescence from Olefins

It is easy to appreciate the potential of the unusual environment of the zeolite, when one realizes that even olefins, systems that under normal conditions do not show phosphorescence, emit from their triplet states when included in  $Tl^{+}$ -exchanged zeolites.

2.2.1. Phosphorescence from Stilbenes

Excitation of (*E*)-stilbene included in TI X and in TI ZSM-5 emits phosphorescence and fluorescence both at room temperature and at 77 K (Fig. 7) [10]. The triplet emission spectra at 77 K for a number of substituted (*E*)-stilbenes included in TI X are provided in Fig. 8. The triplet emission maxima for stilbenes measured in the present study agree well with the literature reports [11]. The ability to record phosphorescence from stilbenes even at room temperature is significant as only very weak phosphorescence from (*E*)-stilbene and several substituted (*E*)-stilbenes have been recorded at 77 K in organic glass containing EtI as the heavy-atom perturber [11].

2.2.2. Phosphorescence from 1-Phenylcycloalkenes and (Benzo)-Fused Cycloalkenes

In an effort to expand the utility of these zeolite hosts for the observation of phosphorescence from triplet states, we have investigated the photophysics of several 1-phenylcycloalkenes and benzo-fused cycloalkenes included in  $Tl^{+}$ -exchanged zeolites. In Fig. 9, the triplet emission spectra at 77 K of several 1-phenylcycloalkenes and benzo-fused cycloalkenes included in TI X are provided [12]. For compounds for which literature estimates are available, the 0-0 transition of the phosphorescence emission and the reported  $S_0$  to  $T_1$  absorption agree remarkably well (see insert in Fig. 9) [13].

2.2.3. Phosphorescence from  $\alpha,\omega$ -Diphenylpolyenes

(all-*E*)- $\alpha,\omega$ -diphenylpolyenes exhibit very low intersystem-crossing efficiencies and efficient fluorescence. To our knowledge, no authentic phosphorescence spectra from these have been reported. We have succeeded in recording phosphorescence of these  $\alpha,\omega$ -diphenylpolyenes by including them in  $Tl^{+}$ -exchanged zeolites [8]. Fig. 10 shows the observed phosphorescence of the  $\alpha,\omega$ -diphenylpolyenes included in TI X. At 77 K, a well-resolved structured emission for each of the polyenes with a prominent vibronic spacing of 1200-1400  $cm^{-1}$  as expected for triplet phosphorescence is observed. The singlet-triplet energy gaps ( $\Delta_{T_1-S_0}$ ) obtained from the observed 0-0 lines are in excel-

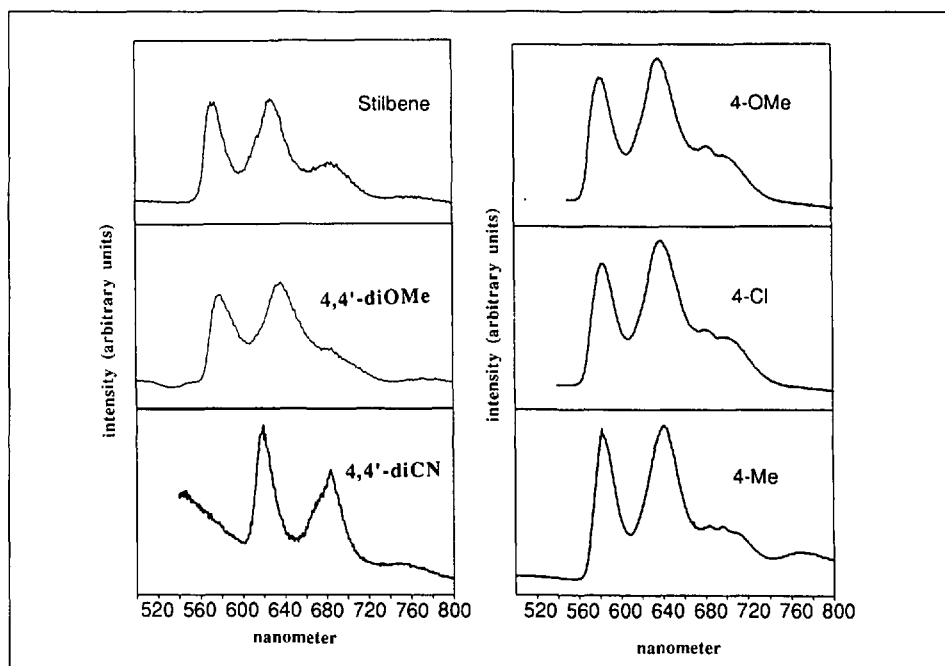


Fig. 8. Phosphorescence spectra at 77 K of para-substituted (*E*)-stilbenes (stilbene; 4,4'-dimethoxy; 4,4'-dicyano; 4-methoxy; 4-chloro; 4-methyl) included in TI X. Excitation wavelength in all cases: 320 nm [12].

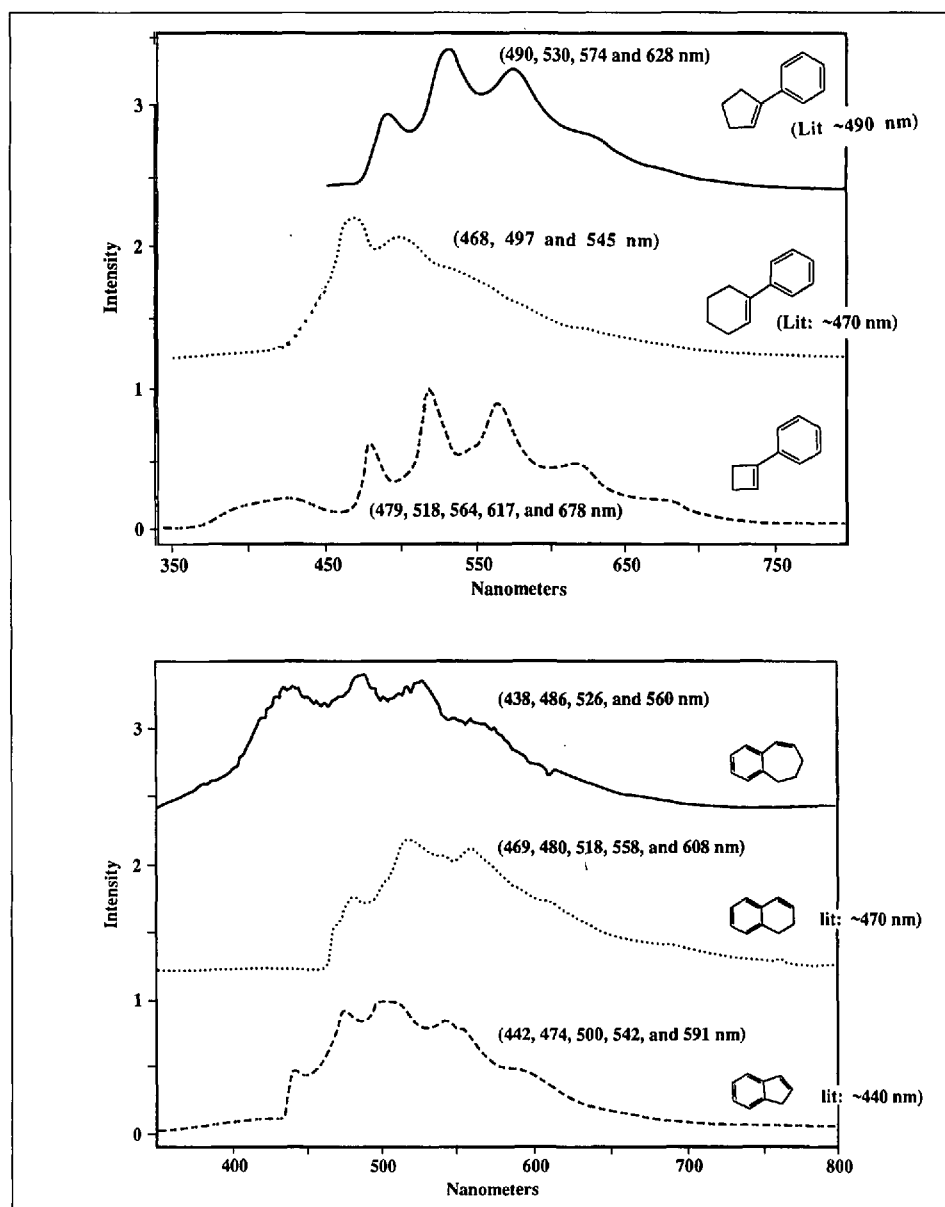


Fig. 9. Phosphorescence spectra at 77 K of 1-phenylcycloalkenes (above) and phenyl fused cycloalkenes (below) included in TI X. Excitation wavelength shown on the Fig. [12].

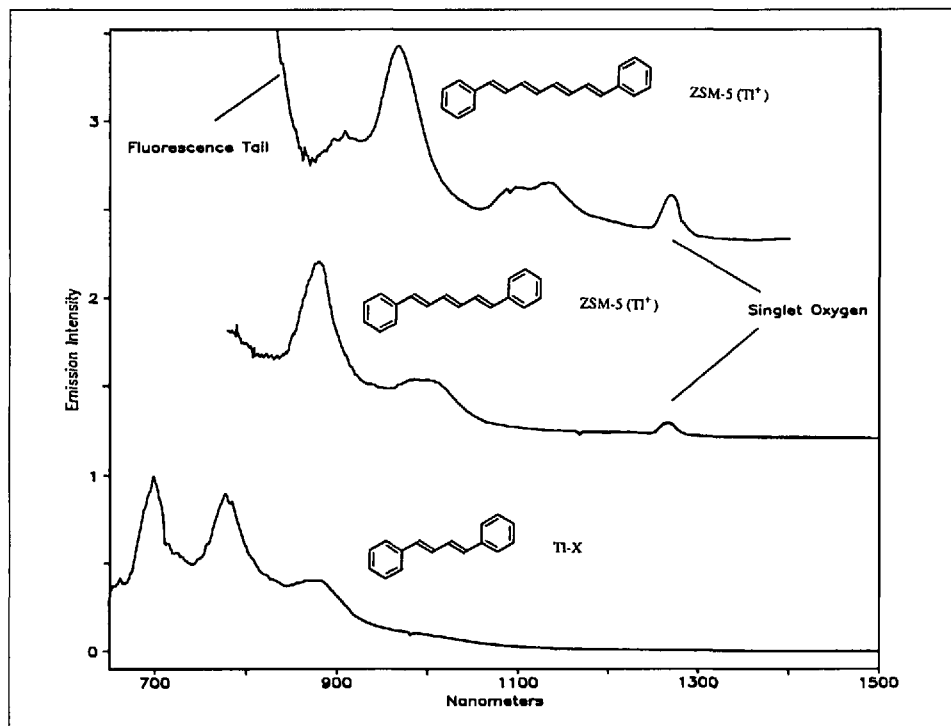


Fig. 10. Phosphorescence spectra at 77 K of  $\alpha,\omega$ -diphenyl polyenes included in TI X. Excitation wavelength: diphenylbutadiene, 340 nm; diphenylhexatriene, 350 nm; diphenyloctatetraene, 375 nm.

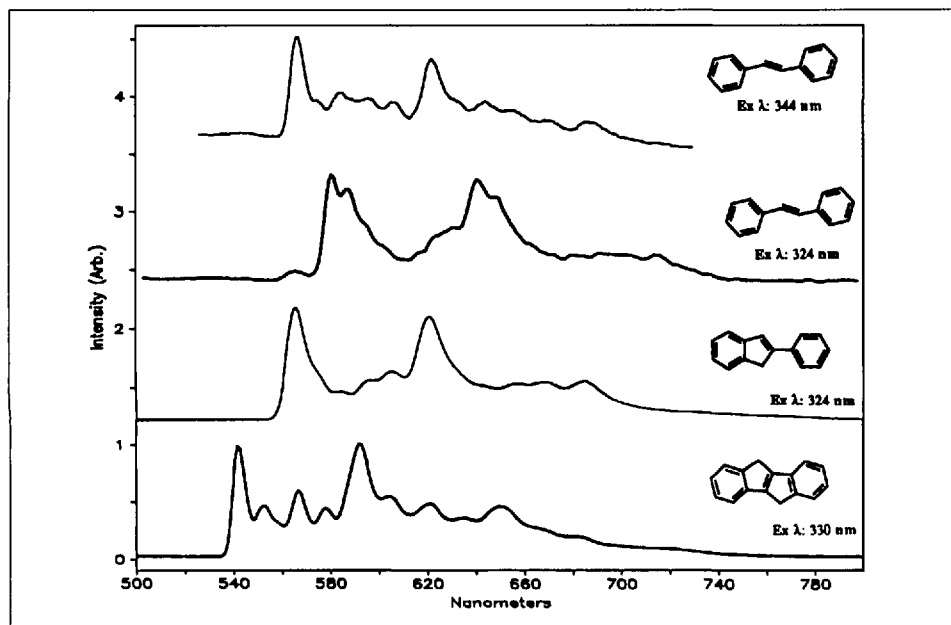
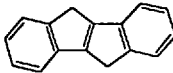

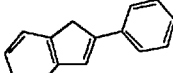

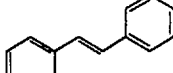
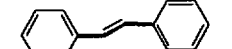


Fig. 11. Phosphorescence spectra at 77 K of (E)-stilbene, phenylindene and indenoidene included in TI X. Excitation wavelengths are shown as inserts. Note the excitation wavelength dependent emission from *trans*-stilbene.

Scheme 1

Phosphorescence $\lambda_{max}$		
	548, 595, 652	
	567, 620, 680	
	580, 636, 698	

lent agreement with literature predictions [14].

2.2.4. Excitation Wavelength and Zeolite Dependent Triplet Emission

The emission maxima were dependent on the excitation wavelength for several olefins when included in either TI X or in TI Y. This was very pronounced for stilbenes and was independent of the temperature in the range 3.4 to 300 K (Fig. 11). It is important to note that the emission spectra significantly changed with a small variation in the excitation wavelength (340–344 nm). Another example, 1,2-dinaphthylethylene, displayed in Fig. 12, also shows wavelength dependent emission (360 vs. 380 nm). These observations suggest that not all molecules of the guest included within X and Y zeolites reside under identical environments.

The triplet emission observed for a number of stilbenes and a few 1,4-diarylbutadienes included in TI ZSM-5 are consistently blue-shifted with respect to the emission monitored in TI X (Fig. 7). A comparison of the maxima for (E)-stilbene with the rigid analogs of (E)-stilbene (Fig. 11), phenylindene, and indenoidene revealed to us that conformations of (E)-stilbene included in TI ZSM-5 are different from the one observed in a glassy matrix. On the basis of the model compounds shown in Scheme 1, we concluded that when (E)-stilbene enters the channels of ZSM-5, it is preferentially included in a conformation in which one of the Ph rings is planar with respect to the central bond, while the other is partially twisted. Similarly, when phenylindene enters the channel, it probably attains a better planarity than is present in solution.

3. Generation, Reactivity, and Photo-physics of Reactive Intermediates within Zeolites

Photochemistry and photophysics of organic reactive intermediates such as radicals, diradicals, radical ions, carbonium ions, carbanions, carbenes, and nitrenes have attracted recent attention [15]. These studies have not become routine in part due to the absence of simple methods of preparing and stabilizing them. Photophysical studies, in general, require two photon time resolved or matrix techniques. Surprisingly, radical ions of organic molecules can be generated and stabilized within zeolites by a simple procedure. Results of this study are summarized below. Observations made although relate directly to radical ions, potential exists for expanding this observation to other reactive intermediates.

### 3.1. Generation of $\alpha,\omega$ -Diphenylpolyene Radical Cations

When activated Na-ZSM-5 (Si/Al = 22) was stirred with  $\alpha,\omega$ -diphenylpolyenes ((*E*)-stilbene, diphenylbutadiene, diphenylhexatriene, diphenyloctatetraene, diphenyldecapentaene, and diphenyldodecahexaene) in 2,2,4-trimethylpentane, the initially white zeolite and colorless to pale-yellow olefins were transformed into highly-colored solid complexes within a few min [16]. The samples all exhibited intense ESR signals with *g* values of 2.0028. Diffuse reflectance spectra of these powders (Figs. 13 and 14) are identical to the spectra of the radical cations of a few  $\alpha,\omega$ -diphenylpolyenes reported in the literature [17]. Diffuse reflectance and ESR results favor the conclusion that the colored species formed upon inclusion of  $\alpha,\omega$ -diphenylpolyenes in Na-ZSM-5 are radical cations.

The colored  $\alpha,\omega$ -diphenylpolyene radical cations generated in the channels of Na-ZSM-5 were found to be unusually stable; even after several weeks storage at ambient temperature in air, the colors persisted, and the peak positions of the diffuse reflectance spectra were unchanged. This is to be contrasted with their short lifetimes in solution ( $\mu$ s) and in solid matrices (s) [17]. The remarkable stability of these radical cations in Na-ZSM-5 derives from the tight fit of the rod-shaped molecules in the narrow zeolite channels; the  $\pi$  orbitals are protected from external reagents by the Ph rings which fit tightly in the channels at both ends of the radical (Fig. 15). By including a number of 4-substituted stilbenes with varying oxidation potentials in the channels of ZSM-5 the redox potential of the zeolite's oxidizing sites has been estimated to be near 1.65 eV vs. SCE. The approximate number of oxidizing sites present in the channels was estimated by carrying out the oxidation at various loading levels and determining the loading range at which all of the adsorbed polyenes were oxidized. The limiting loading level at which all the included diphenylhexatriene and diphenyloctatetraene were oxidized corresponded to ca. 0.005 mg ( $\sim 2 \times 10^{-7}$  M) per g of zeolite. This corresponds to ca. 0.1% of the total loading capacity.

With respect to the nature of oxidizing sites, only limited information is available. Since several alkali cation (Li, K, Cs, and Tl) exchanged ZSM-5 zeolites (Si/Al~22) were effective as oxidants, the cation is not expected to play any pivotal role in the oxidation process. By including the above polyenes in ZSM-5 zeolites with different Si/Al ratios (ranging from 22 to 550), we could conclude that the presence of aluminum in the matrix is

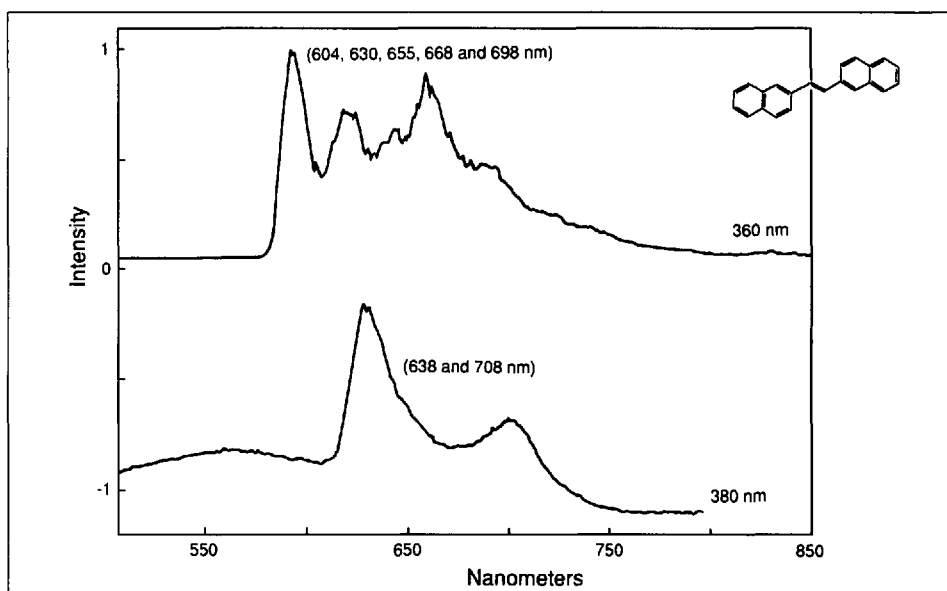


Fig. 12. Phosphorescence spectra at 77 K of (*E*)-1,2-dinaphthylethylene included in Tl X. Excitation wavelength and emission maxima are indicated on the spectra. Note the excitation wavelength dependent emission [12].

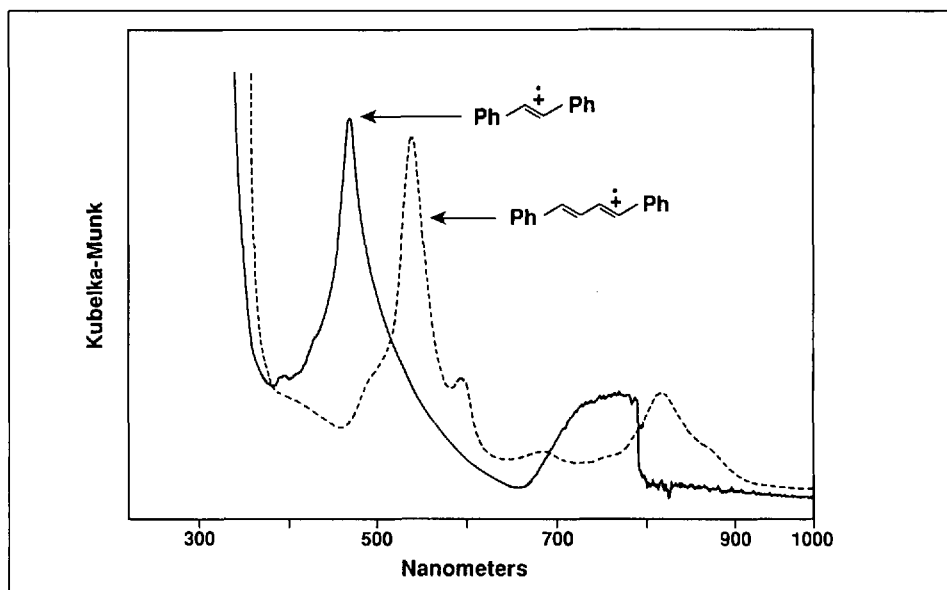


Fig. 13. Room temperature diffuse reflectance spectra of the cation radicals of stilbene and diphenylbutadiene generated via inclusion in activated Na-ZSM-5

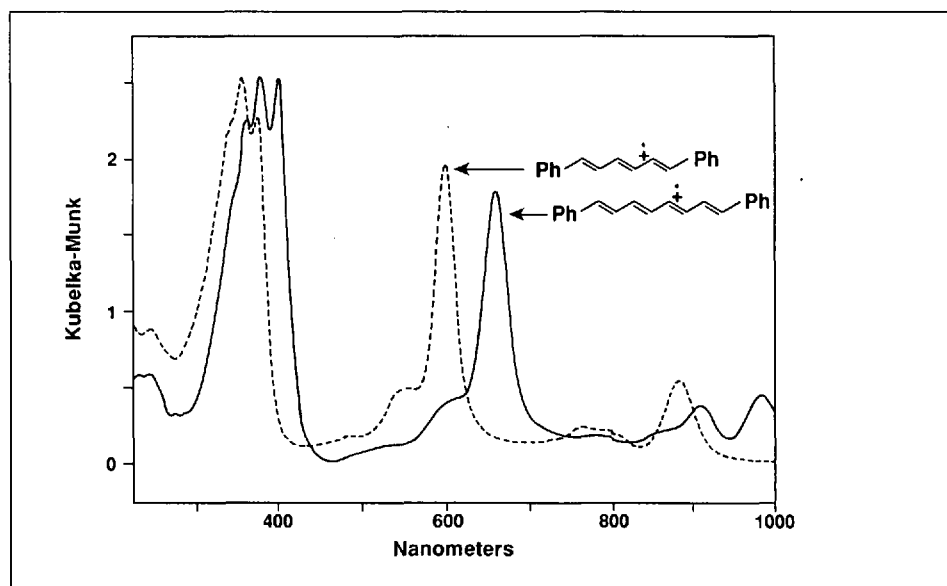


Fig. 14. Room temperature diffuse reflectance spectra of the radical cations of diphenylhexatriene and diphenyloctatetraene generated and stabilized within Na ZSM-5

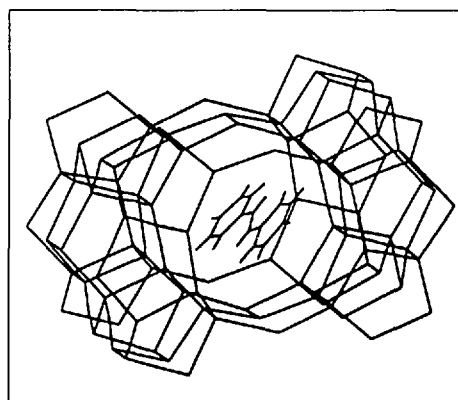


Fig. 15. Model showing the structure of (E)-stilbene included in the channels of ZSM-5. The view is along the direction of the straight channel (crystallographic b-axis).

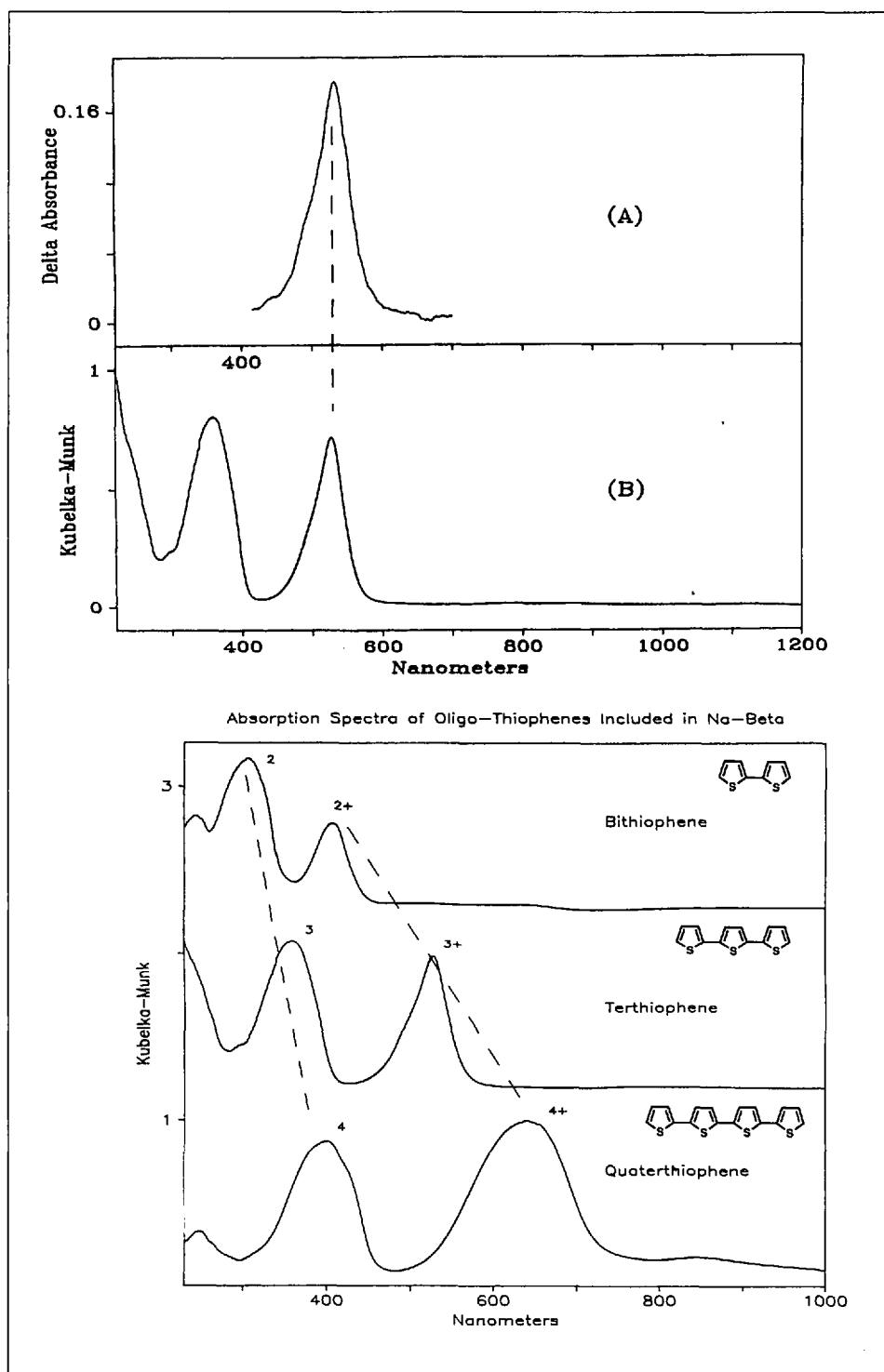


Fig. 16. Top: A) The absorption spectrum of the cation radical of terthiophene generated by flash photolysis as a solution transient. Data taken from [22]. B) Room temperature diffuse reflectance spectrum of terthiophene, included in Na- $\beta$  showing the formation of the cation radical of terthiophene. Bottom: Room temperature diffuse reflectance spectra of bithiophene, terthiophene and quaterthiophene included in Na- $\beta$ . Transitions due to the neutrals and cation radicals are labeled [21].

essential. Purely silicious ZSM-5 (Si/Al $\approx$ 550) was found to be completely inactive. It is not clear at this stage what role aluminum plays in the oxidation process. One possibility is that some type of aluminum containing defect site is acting as the oxidant. The generality of this chemistry has been explored by surveying a number of common zeolite hosts. We find that oxidation is observed with ZSM-8 and ZSM-11, while no reactivity is detectable for NaX, NaY, M-5,  $\Omega$ -5, LZ-L, or ZSM-34 [18].

### 3.2. Reactivity of Radical Cations within Zeolites: Formation of Cation Radical and Dication of Oligothiophenes

When either activated Na- $\beta$  or NaZSM-5 (Si/Al $\approx$ 22) was loaded with terthiophene, a deep red-purple complex was obtained [19]. Comparison of the diffuse reflectance spectrum of the above deep red-purple complex with flash photolysis results, where the terthiophene cation radical is generated as a transient in solution, shows excellent agreement (Fig. 16) [20]. As expected for a simple cation radical, an EPR spectrum for the above complex was observed although no hyperfine structure was resolved. The results obtained for terthiophene included in Na- $\beta$  and NaZSM-5 are not unique. The same type of one electron oxidation reaction for bithiophene and quaterthiophene included in either ZSM-5 or Na- $\beta$  was observed (Fig. 16). The stability of the cation radicals, which exist only as reactive intermediates in solution, is very much higher within the zeolite channels; we have stored samples of the terthiophene cation radicals for months without any significant degradation (except as noted below) even in the presence of air and water. However, most interesting aspect of this study relates to the reactivity of these radical cations in the channels of ZSM-5. On standing at room temperature or with mild heating (60–140 $^\circ$ ), new bands appear at longer wavelengths in the diffuse reflectance spectrum (Fig. 17). These bands are due not to decomposition of the cation radical, but rather are due to further oligomerization. The complex appearance of the spectra in Fig. 17 is the result of the presence of neutral, cation radical, and dications of terthiophene and its higher oligomers. Prolonged heating of the above sample results in the formation of the doped polythiophene. Slow polymerization observed in the ZSM channel provided an opportunity to follow the oligomerization of thiophenes. Earlier attempts to follow the oligomerization of thiophenes by other techniques have failed [21]. In all of these cases, the polymerization could not be



controlled and could not be stopped at the stage of oligomers. Two approaches, 'multiplication of original chain length' and 'selective methylation' which are briefly sketched in *Scheme 2* were used to assign the transitions present in the diffuse reflectance spectra recorded during the oligomerization of bi-, tri-, or tetrathiophene in the channels of ZSM-5. For details of assignment of the transitions of the various oligomeric thiophene radical ions and dications, readers are referred to the original paper. It should also be noted that the transitions are assigned on the basis of the 'band model' shown in *Fig. 18* [22].

The results of the assignment of transitions for thiophenes with chain lengths between 2 and 9 are summarized in *Table 3*. The peak positions for the neutral oligomers, polarons, and bipolarons all vary in a systematic manner with inverse chain length as shown in *Fig. 19*. This dependence appears to be a manifestation of the well known reciprocal rule for polymers which has been observed previously both experimentally and theoretically for the band-gap absorption of neutral thiophene oligomers. To our knowledge, this is the first experimental observation of this phenomenon for polarons and bipolarons of conducting polymers. Detailed analysis of these dependences provides useful predictions of properties of bulk doped polythiophene [23]. Excellent agreement for the electronic transitions of doped polythiophene between the literature values and predicted values based on the above correlation is observed (*Fig. 19*). If thiophene oligomers are to be considered as a model for doped polythiophene, cation radicals of  $\alpha,\omega$ -diphenylpolyenes discussed in *Sect. 3.1* should serve as a model for polyacetylene [24]. Indeed as shown in *Fig. 20* a linear relationship between the electronic transitions of the  $\alpha,\omega$ -diphenylpolyene radical cation and the chain length is observed; the extrapolated transition in fact corresponds to the literature value of polyacetylene absorption [25][26]. For the first time, the evolution of the electronic structure of doped polythiophene and polyacetylene from monomer to polymer has been observed directly for chain lengths between 2 and 9, and this is made possible by the unique features of the zeolite medium.

#### 4. Zeolite as a Photochemical Reaction Cavity

Photoreactions, over the last decade, has been investigated in a number of organized media [1]. A unified model should aid the understanding and predicting the behavior of molecules in different media.

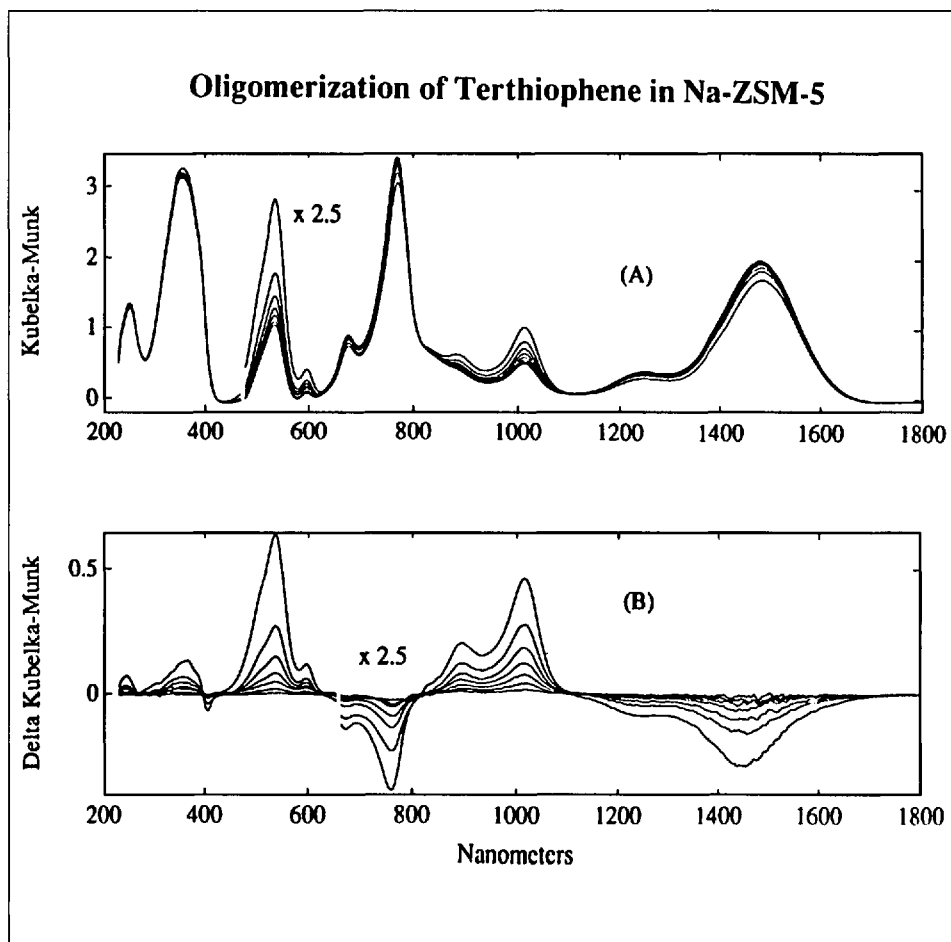
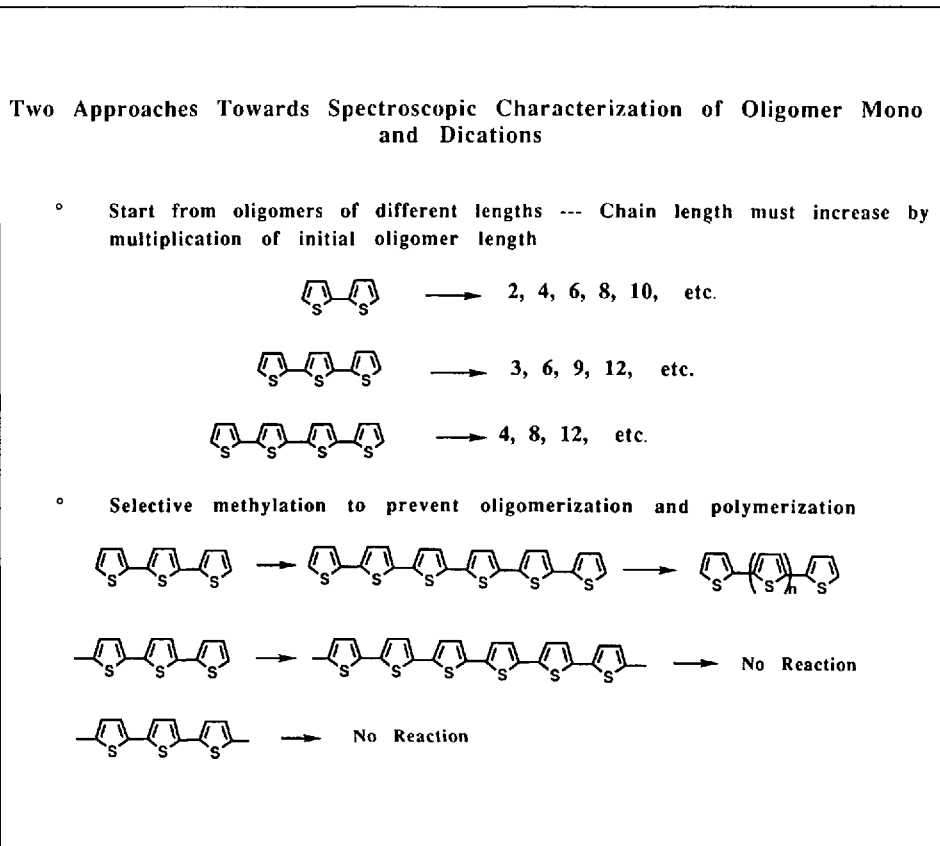


Fig. 17. A) Room temperature diffuse reflectance difference spectra of terthiophene included in ZSM-5 recorded at 2 h intervals. B) Difference spectra for the series of scans in (A) presented as  $R-R_{\infty}$  where  $R_{\infty}$  is the reflectance of the final scan. Peaks above zero are due to species whose concentrations are decreasing with reaction time and those below zero are increasing with reaction time. The reaction was followed to very near completion (at r.t.). An additional scan made after a further 24 h of reaction was indistinguishable from the scan after 18 h [21].

Scheme 2



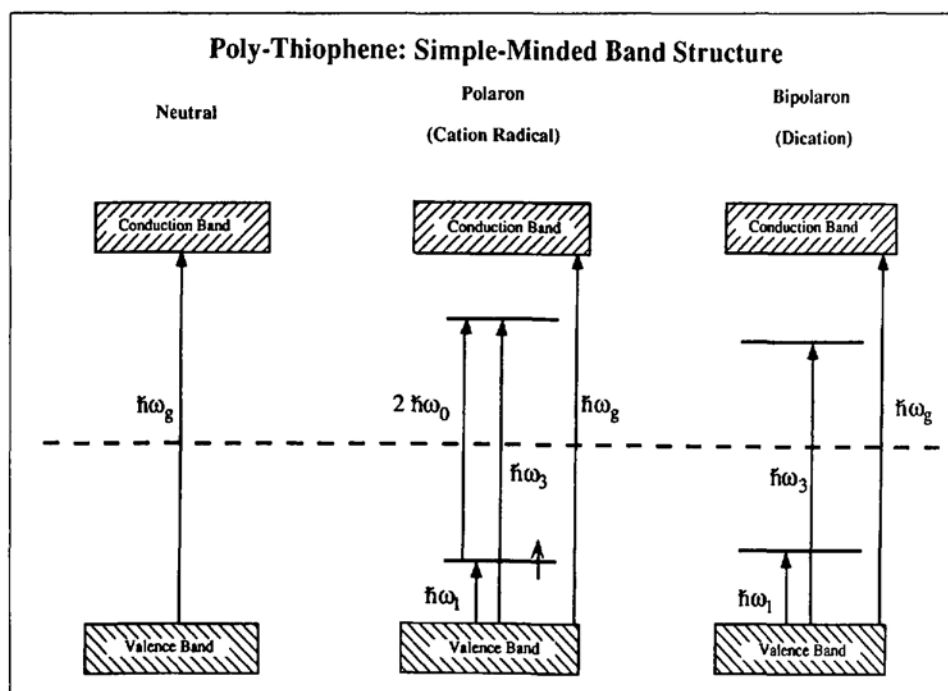


Fig. 18. Simple band picture for the oxidative doping of polythiophene [21]

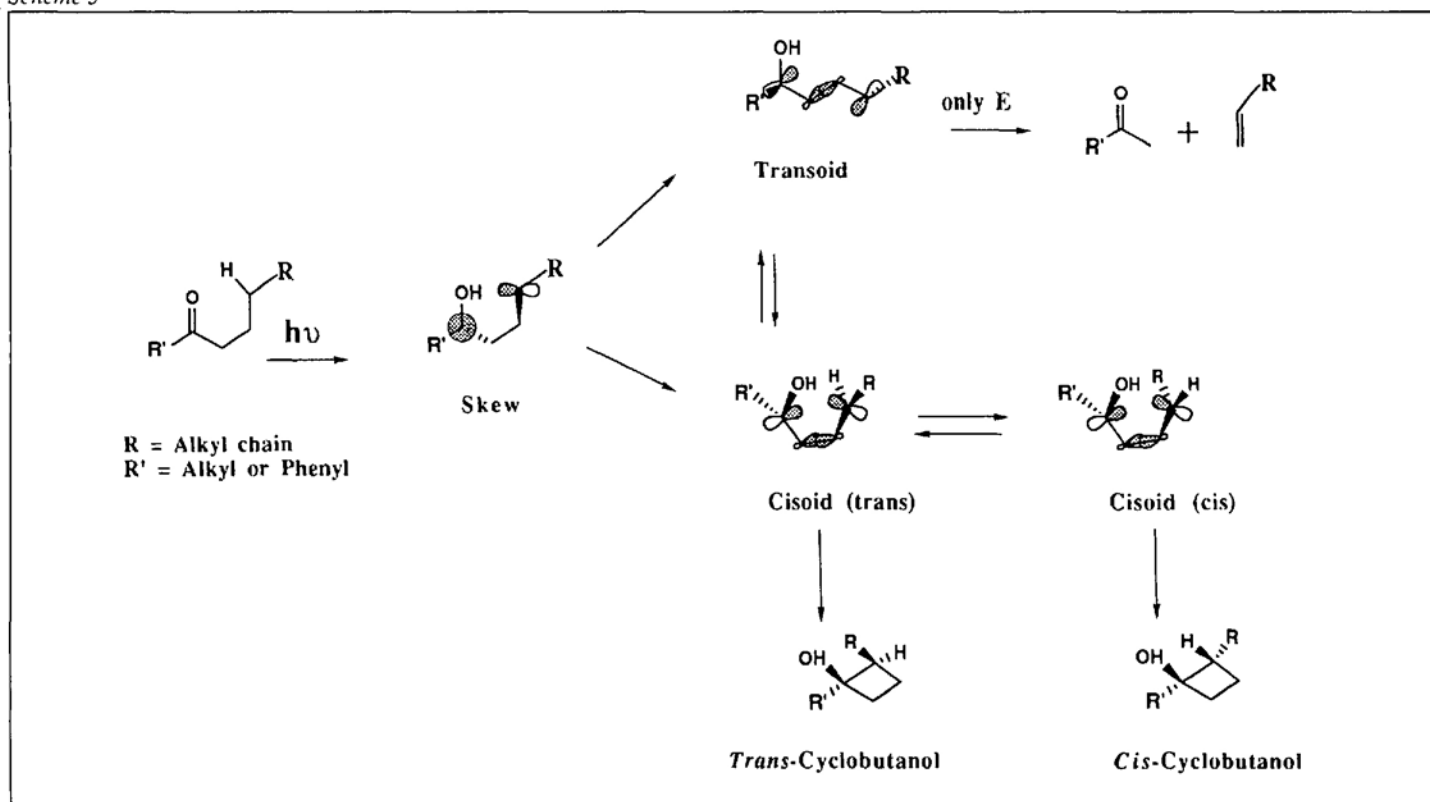
Table 3. Electronic Absorption Band Positions for Oligomeric Thiophenes ( $2 \leq n \leq 9$ ) Included in Na-ZSM-5. The positions cited are the peak maxima in nm for the 0-0 vibronic transitions observed in r.t. diffuse reflectance spectra.

Oligomer Chain Length	$h\bar{\omega}_g$ (Neutral)	$2h\bar{\omega}_0$ (Polaron)	$h\bar{\omega}_3$ (Bipolaron)	$h\bar{\omega}_1$ (Bipolaron)
2	300	407	-	-
3	354	522	-	833
4	390	614	636	1046
6	434	775	600	1019
8	-	-	661	1383
9	-	-	761	1450

We believe that the 'reaction cavity' concept originally due to *Cohen* should be of some value in this context [27]. The reaction cavity is the space occupied by the reacting partners and the empty region (area or volume) surrounding them (Fig. 21). Differences in product selectivity obtained for a particular reaction between various media can be attributed to the size, shape, and nature (texture or flexibility) of the reaction cavity available for the reactant molecules. The degree of tolerance of the 'reaction cavity' to the distortions that accompany a reaction is expected to play an important role in the extent of selectivity obtained. Organic solvents have served as a medium for reactions for over a century. Very little selectivity is obtained in this medium, as it totally responds to the shape changes that occur in a 'reaction cavity' as the reaction proceeds. On the other hand, organic crystals which do not tolerate any shape changes do not serve as a medium for a large number of reactions, although selectivity in a few cases where it serves as a medium is impressively high [28]. To generalize the use of organized structures as a medium for photoreactions, one has to establish the connection between the selectivity and the features (size and texture) of the 'reaction cavity'. In this section, we explore the relationship between the selectivity in a photoreaction and the characteristics of the 'reaction cavity'.

In this study, the size of the 'reaction cavity' is varied by two approaches. In one, zeolites with different internal struc-

Scheme 3



tures are chosen. The internal structure of the two types of zeolites (faujasites: X and Y and pentasils: ZSM-5 and ZSM-11) that we have utilized as media vary significantly in size and shape (Fig. 1). In the second approach, the same zeolite with different alkali cations are utilized. Results presented below brings out a powerful message that, in order to obtain a high product selectivity, one should utilize a reaction cavity that is large enough to respond to the shape changes that occur along the reaction coordinate but at the same time hard and small enough to provide relatively different extents of restriction on various reaction pathways available to the reactive intermediates.

#### 4.1. Cavity-Size Control by the Choice of Zeolite

##### 4.1.1. Norrish Type II Reaction of Alkyl Aryl Ketones and Alkanones

The Norrish type-II reaction of ketones has been extensively investigated, and the mechanistic details are fairly well understood [29]. The triplet 1,4-diradical, the primary product of  $\gamma$ -H abstraction is generated in the skew form and transforms to the *transoid*- and *cisoid*-conformers via a rotation of the central  $\sigma$  bond (Scheme 3). As illustrated in Scheme 3, these *cisoid*- and *transoid*-conformers undergo further reaction to yield cyclobutanol, olefin, and enol as final products. While the *cisoid*-conformer reacts via both elimination and cyclization processes, the *transoid*-conformer undergoes only elimination. The skew diradical can also directly give rise to products via elimination and cyclization processes, and this is determined by how easily the required orbital overlap can be attained and by how readily the accompanying atomic motions can be tolerated by the medium and by the molecular architecture. The stereochemistry of the cyclobutanols (*cis* and *trans*) is determined by the population and decay of the two *cisoid*-biradicals depicted in Scheme 3. One can understand the influence of the 'micro-environment' on the type-II cyclization and elimination ratio (E/C) and on the *trans/cis*-cyclobutanol ratio on the basis of the medium effect on the equilibrium distribution and decay of the *cisoid*- and *transoid*-1,4-diradical conformers.

Photolysis of alkyl aryl ketones such as valerophenone, octanophenone, and other higher analogs included in pentasil zeolites (ZSM-5 and ZSM-11) give via the Norrish type-II process only elimination products, although both cyclization and elimination products are obtained in faujasites and in isotropic solution media (Table 4) [30]. The fact that the type-II reaction is observed in ZSM-5 indicates that the smaller reaction cavity ( $\sim 5.5$  Å

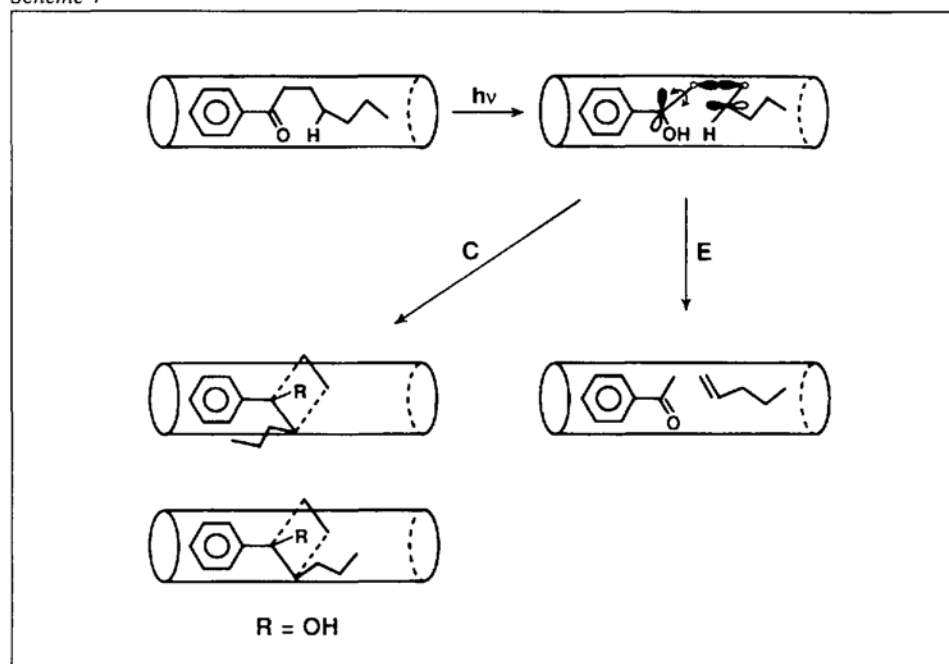
Table 4. Elimination (Olefin and Alkanone of Shorter Chain Length) to Cyclization (*cis*- and *trans*-Cyclobutanols) Product Ratio upon Photolysis of Alkyl Aryl Ketones and Alkanones in Zeolites

S. No.	Alkanones	Hexane	Na X	NaY	ZSM-5	ZSM-11
1	Valerophenone	2.8	1.2	1.1	only E	only E
2	Octanophenone	1.8	0.9	0.6	only E	only E
3	Dodecanophenone	1.8	0.6	0.5	only E	only E
4	Tetradecanophenone	3.5	0.5	0.2	only E	only E
5	2-Tridecanone	2.8	1.0	0.9	4.3	4.5
6	4-Tridecanone	1.9	0.3	0.5	4.0	4.1
7	6-Tridecanone	1.6	0.7	0.8	2.7	3.2
8	4-Tetradecanone	1.9	0.4	0.7	3.3	4.1
9	5-Decanone	1.3	1.0	0.8	3.0	3.5

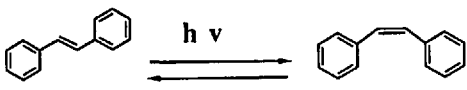
Table 5. *trans*- to *cis*-Cyclobutanol Ratio upon Irradiation of Alkanones in Zeolites

S.No	Alkanones	Hexane	Na X	NaY	ZSM-5	ZSM-11
1	4-Nonanone	1.8	0.6	1.3	60	60
2	4-Undecanone	1.8	0.4	0.7	60	60
3	4-Dodecanone	1.7	0.7	0.9	65	70
4	4-Tridecanone	1.7	0.7	1.1	70	68
5	4-Tetradecanone	1.7	0.8	1.1	72	66
6	4-Decanone	1.8	0.4	0.7	60	60
7	3-Decanone	1.8	0.4	0.9	16	14
8	2-Decanone	1.5	0.6	1.0	6.0	6.5
9	3-Octanone	1.8	0.7	0.8	20	18
10	4-Octanone	1.8	0.7	1.3	15	18
11	2-Octanone	1.4	0.8	1.2	8.0	7.1
12	2-Heptanone	1.7	0.8	0.9	3.8	4.1
13	3-Heptanone	1.5	0.6	0.9	2.8	2.6
14	2-Hexanone	1.5	0.8	1.3	2.4	2.7

Scheme 4

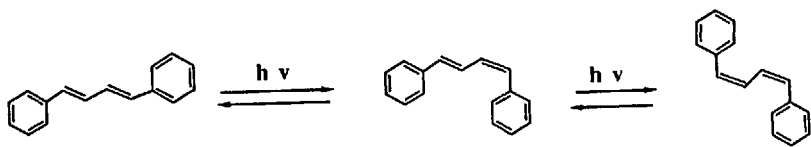


Scheme 5



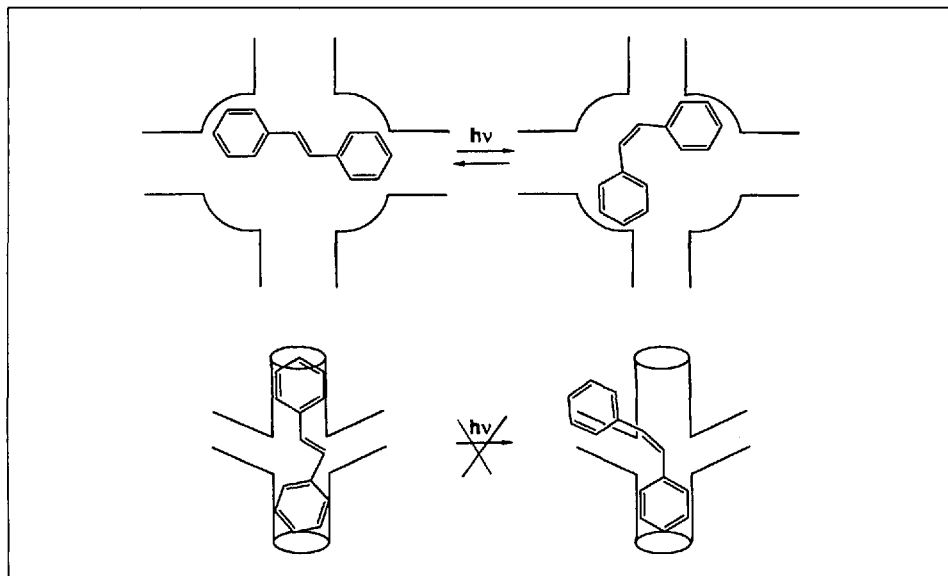
Medium	Initial	Photostationary state mixture	
		trans	cis
Benzene	trans	28	72
	cis	26	74
Li-X	trans	56	44
	cis	12	88
Cs-X	trans	73	27
	cis	34	66
ZSM-5	trans	100	--
ZSM-8	trans	100	--
ZSM-11	trans	100	--

Scheme 6



Medium	Initial	Photostationary state		
		trans,trans	trans,cis	cis,cis
Benzene	trans,trans	18	75	6
	trans,cis	17	76	7
Li-X	trans,trans	76	20	3
	trans,cis	41	45	12
Cs-X	trans,trans	73	17	10
	trans,cis	35	44	20
ZSM-5	trans,trans	100	-	-
ZSM-8	trans,trans	100	-	-
ZSM-11	trans,trans	100	-	-

Scheme 7



diameter) hinders but does not completely prevent the attainment of the required geometry for H abstraction by the triplet ketone. The preference for elimination process in pentasils can be understood on the basis that the relatively large motions required for the conversion of the skew diradical to cyclobutanols either directly or via the *cisoid*-diradicals are not tolerated by the narrow channels of pentasils (Scheme 4). Such a model would predict that the relative size of the channel to the reactant will play a crucial role in product selectivity. Results on alkanones validates the above prediction [31]. A number of alkanones where the bulky Ph group in alkyl aryl ketone is replaced by a long alkyl chain were irradiated in hexane, as included in faujasites (Na X and Na Y) and in pentasils (ZSM-5 and ZSM-11). In all cases both fragmentation (olefin and alkanone of shorter chain length) and cyclization products (*cis*- and *trans*-cyclobutanols) from the initial 1,4-diradical are obtained. The results presented for alkanones in Table 4 contrasts sharply with that of alkyl aryl ketones. The formation of cyclobutanols from alkanones clearly is a reflection of the relative cavity size with respect to the reactant. In the narrow channels of pentasils, alkyl aryl ketones ( $d \approx 5.5 \text{ \AA}$ ) is expected to be held tightly with little space around the reaction center. On the other hand, alkanones ( $d \approx 4 \text{ \AA}$ ) when placed in the channels of pentasils will leave some space around them. This vacant space would be sufficient to permit the motions required for the formation of the *cisoid*-diradical (and cyclobutanol) from the primary skew 1,4-diradical (Scheme 3).

Most interesting results come from the selectivity seen between the *cis*- and the *trans*-cyclobutanols in the channels of pentasils (Table 5) [31]. Both *trans*- and *cis*-cyclobutanols are obtained from all the 14 alkanones, when they are irradiated in hexane, Na X and Na Y, with the ratio differing slightly between the three media. However, in pentasils the ratio of *trans*- to *cis*-cyclobutanols, depending on the alkanone, differed dramatically from those in the above three media. *trans*-Cyclobutanol was preferentially obtained in the case of 4-alkanones (Table 5, see Nos. 1-5). The ratio *trans/cis* over 50 corresponds to less than 2% of the *cis*-isomer. Such a preference for the *trans*-cyclobutanol in the channels of ZSM-5 and ZSM-11 is believed to result from the differences in size and shape of the two isomers and their diradical precursors. Between the *trans*- and the *cis*-cyclobutanol and their precursor diradicals, the *cis*-isomer and its precursor 1,4-diradical possess shape and size which are relatively large to fit into the channels. Consequently, the *trans*-cyclo-

butanol is favored. On the basis of the above argument, one would expect the alkanones, in which the *trans*- and the *cis*-cyclobutanols have closely similar shape and size, to yield *cis*-cyclobutanol along with the *trans*-isomer. This is certainly the case. Alkanones such as hexanone, heptanones, and octanones (Table 5, see Nos. 9–14) give both *trans*- and *cis*-cyclobutanols. It is of interest to note that there is a correlation between the size or length of the alkyl chain and the selectivity: octanone > heptanone > hexanone. Such a trend is also seen with 2-, 3-, and 4-substituted decanones (Table 5, see Nos. 6–8). When the carbonyl substitution is moved along the chain (2-, 3-, and 4- positions) one generates a *cis*-cyclobutanol of increasing bulkiness. The fact that the selectivity for the *trans*-isomer increases with the bulkiness of the *cis*-cyclobutanol (from 2- > 3- > 4-decanones) further confirms our model that relative size of the reactant to the reaction cavity is an important parameter to be considered.

4.1.2. Geometric Isomerization of Olefins

The importance of free volume and the size of the reaction cavity on photoreactions is further probed by examining the geometric isomerization of olefins, a volume-demanding photoreaction, in the cages/channels of zeolites [32]. While both (*Z*)- and (*E*)-stilbene can be included into faujasites, only the latter was accommodated by pentasils. A similar difference in inclusion was noticed between (*E,E*)- and (*E,Z*)-1,4-diphenylbutadienes. This is not surprising considering the channel size of pentasils and the molecular size and shape of the (*Z*)-isomers. Selectivity in inclusion is also reflected in the photobehavior of

Table 6. Consequence of Rotational Restriction on Excited Singlet State Lifetime at Room Temperature

	Medium	Lifetime [ns] <sup>a)</sup>
<i>(E)</i> -Stilbene	Methylcyclohexane	0.11 <sup>b)</sup>
	Na-X	0.21(96%); 4.6(4%)
	Na-Y	0.20(98%); 4.7(2%)
	ZSM-5	1.88
	ZSM-8	1.87
	ZSM-11	3.80
	crystal	6.0
<i>(E,E)</i> -1,4-Diphenylbutadiene	Methylcyclohexane	0.58 <sup>c)</sup>
	Na-X	0.60
	Na-Y	0.67
	ZSM-5	12.7
	ZSM-8	15.1
	ZSM-11	13.2
	Molecular beam jet(4.2 K)	16.0

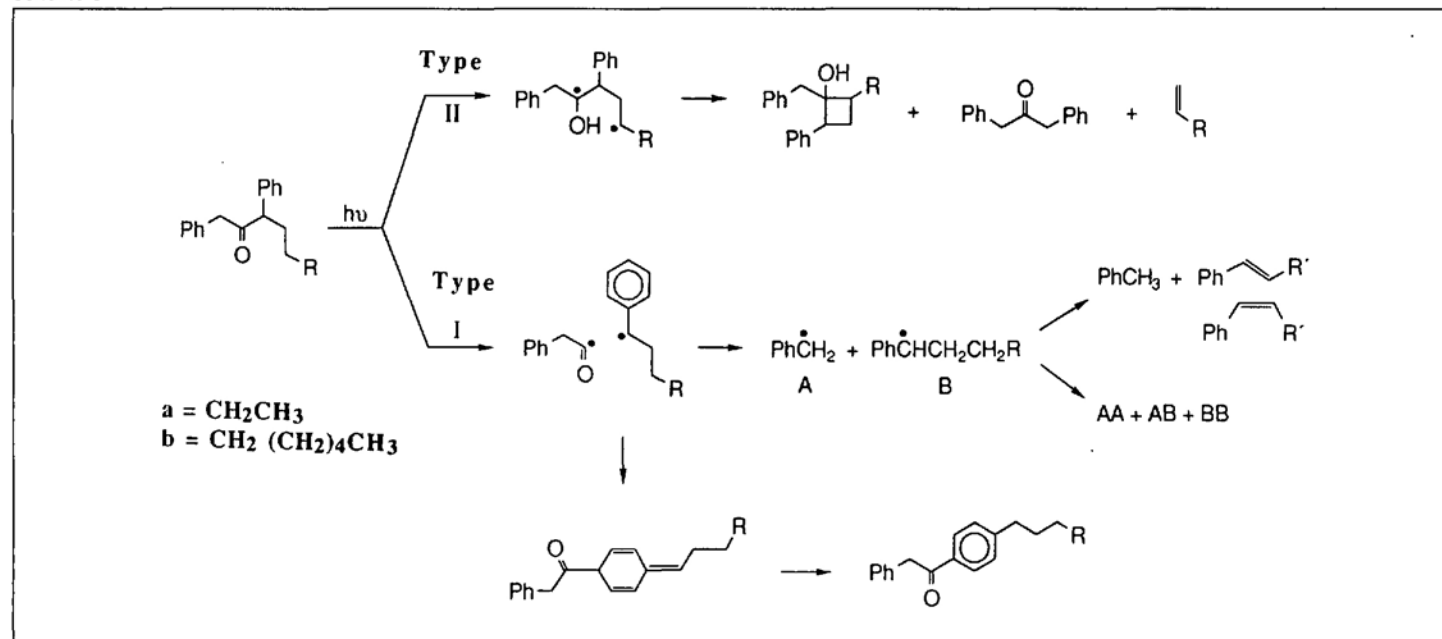
<sup>a)</sup> Excited-state singlet lifetime as measured by a single photon counting apparatus.  
<sup>b)</sup> From M. Sumitani, N. Nakashima, K. Yoshihara, S. Nagakura, *Chem. Phys. Lett.* **1977**, *51*, 183.  
<sup>c)</sup> From P. Reyniers, H. Dreeskamp, W. Kuhmle, K.A. Zachariasse, *J. Phys. Chem.* **1987**, *91*, 3982.

Table 7. Dependence of the Physical Parameters of M Y Zeolites on the Cation

Cation [M <sup>+</sup> ]	Ionic Radius of the Cation [Å] <sup>a)</sup>	Vacant Space <sup>b)</sup> within the Supercage [Å <sup>3</sup> ]	
		Y Zeolite	X Zeolite
Li	0.6	834	873
Na	0.95	827	852
K	1.33	807	800
Rb	1.48	796	770
Cs	1.69	781	732

<sup>a)</sup> R.J. Ward, *J. Catal.* **1968**, *10*, 34.  
<sup>b)</sup> Calculations of polyhedral volumes were performed using a modification of the POLYVOL Program [D. Swanson, R.C. Peterson, *Can. Mineralogist* **1980**, *18*, 153; D.K. Swanson, R.C. Peterson, POLYVOL Program Documentation, Virginia Polytechnic Institute, Blacksburg, VA] assuming the radius of the TO<sub>2</sub> unit to be 2.08 Å (equivalent to that of quartz).

Scheme 8



the included polyenes (Schemes 5 and 6). Direct excitation of the (*E*)-stilbene and (all-*E*)-diphenylbutadiene incorporated in pentasils resulted in no change suggesting that their inclusion in pentasils fully arrested the rotation of ' $\pi$ ' bonds (Scheme 7). However, both the (*E*)- and the (*Z*)-isomers underwent geometric isomerization inside the supercages of faujasites. The above restriction of molecular motion is also indicated by drastic changes in the photophysical properties of the included

guests. In the extremely confining space of the pentasil channels, the polyenes examined all exhibit enhanced fluorescence lifetimes (Table 6). Such lifetimes are significantly longer than in fluid solution or in the supercages of faujasites. For (*E,E*)-1,4-diphenylbutadiene the longest lifetime observed, 16 ns in ZSM-8, is identical within errors to the lifetime observed in a molecular beam experiment where the equivalent temperature is 4.2 K. This similarity emphasizes the rigidity of

the zeolite environment. Likewise, for (*E*)-stilbene in ZSMs the observed lifetimes approach those of rigid analogues. The enhanced lifetime is a direct reflection of the constraint provided by the host which prevents  $\pi$ -bond rotation.

#### 4.2. Cavity-Size Control by the Choice of Cation-Norrish Type-I Reaction

One can control the size of the 'reaction cavity' within a supercage by changing the alkali cation. The free volume

Fig. 19. Plot of the dependence of electronic absorption band energies for oligomeric thiophenes as a function of the inverse chain length,  $n^{-1}$ . A): (X)  $h\omega_g$  for neutral oligomers in solution. ( $\blacklozenge$ )  $2h\omega$  for polarons included in Na-ZSM-5; B) (filled squares)  $h\omega_1$  for bipolarons included in Na-ZSM-5. (filled  $\Delta$ )  $h\omega_3$  for bipolarons included in Na-ZSM-5. ( $\Delta$ )  $h\omega_1 + h\omega_3$  for bipolarons included in ZSM-5-3. The dashed line in (B) is the least squares line for the neutrals in (A).

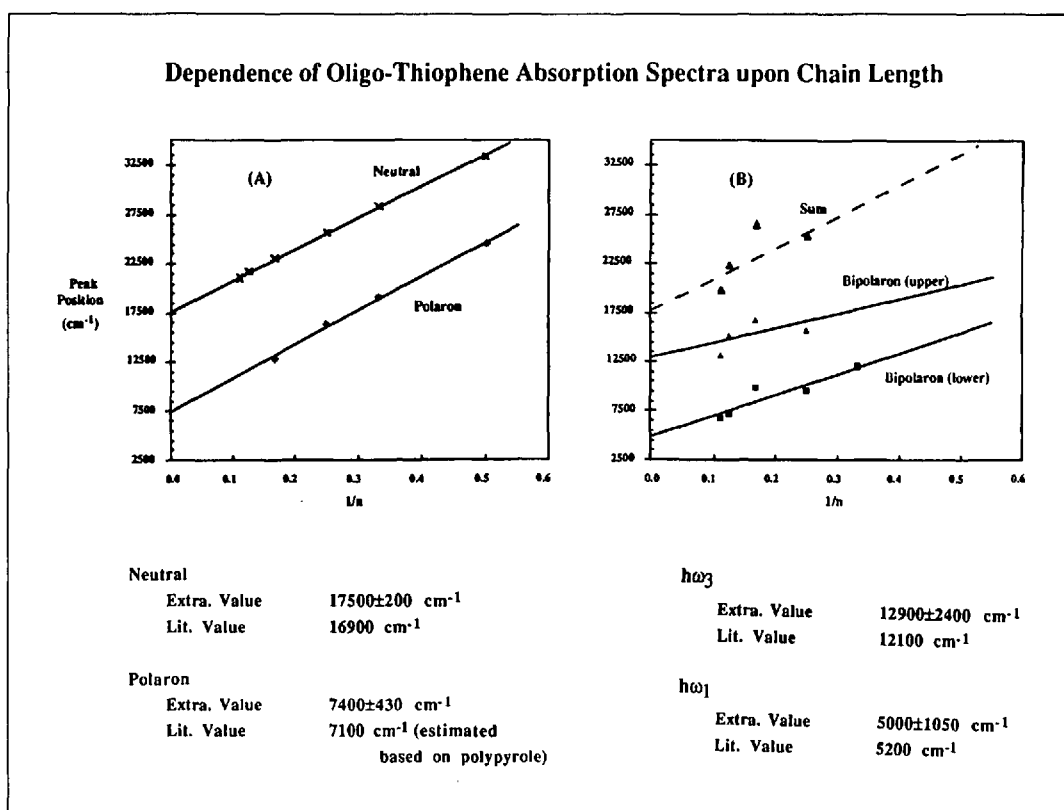
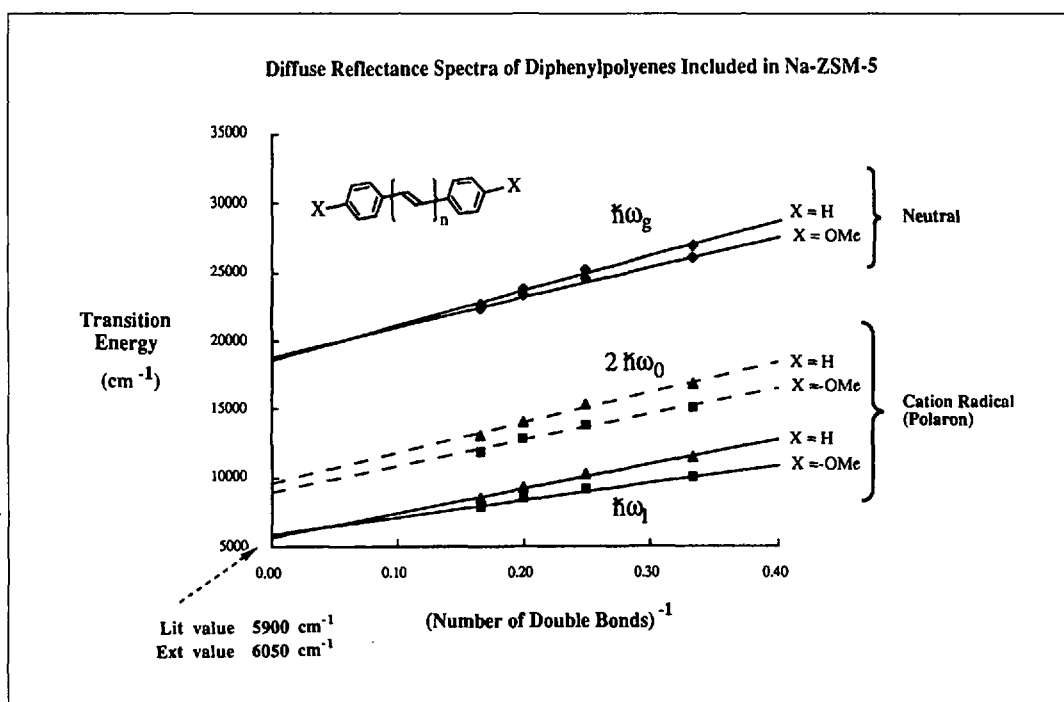


Fig. 20. Plot of the dependence of electronic absorption band energies for cation radicals of  $\alpha,\omega$ -diphenylpolyenes and  $\alpha,\omega,p,p'$ -dimethoxy diphenylpolyenes as a function of the inverse number of double bonds,  $n^{-1}$



available for the organic guest molecule within the supercages of faujasites depends on the number and nature of the cation [3]. As the calculated supercage volumes given in Table 7 for X and Y zeolites show, the free volume decreases as the cation size increases from Li to Cs. This is schematically shown in Fig. 22. Examples provided below from our own studies illustrate the importance of the size of the cation (present within a cage along with the organic guest molecule) on the product distribution [33][34].

Photolysis of  $\alpha$ -alkyl dibenzyl ketones yield a number of products as shown in Scheme 8. In solution, the termination process of the benzyl radicals derived from  $\alpha$ -alkyl dibenzyl ketones consists *only* of the coupling between the two benzylic radicals and results in diphenylalkanes AA, AB, and BB in a statistical ratio of 1:2:1. Within the supercages of X and Y zeolites, on the other hand, termination occurs by *both* coupling and disproportionation, the latter yielding the olefins [33]. The ability of the disproportionation process to compete with coupling within a supercage is attributed to the differences in motions executed during these two processes (Scheme 9). Relatively large overall motion would be required to bring benzylic radicals together for head-to-head coupling than to move an alkyl group so that one of its methylene H-atoms would be in a position for abstraction by the benzylic carbon radical. It is logical to expect the radical pair to prefer the pathway of 'least volume and motion', when the free space around it is small. This model predicts that there should be an inverse linear relationship between the reaction cavity size (or super cage free volume) and the yield of the disproportionation products. Indeed, this is found to be the case (Fig. 23).

The above conclusion is also supported by the pathways undertaken by the primary triplet radical pair (Schemes 8 and 10) generated by the  $\alpha$ -cleavage of the  $\alpha$ -alkyl dibenzyl ketones and  $\alpha$ -alkyl benzoin ethers and deoxybenzoins [33][34]. Perusal of Fig. 24 reveals that while the rearrangement takes place in all cation-exchanged X and Y zeolites, the yield of the rearrangement product varies depending on the cation. The yield decreases, as the cation present in the supercage is changed from Li<sup>+</sup> to Cs<sup>+</sup>. Such a trend is attributed to the decrease in the free space (reaction cavity size) within the supercage. As the available free space inside the supercage is decreased by the increase in the size of the cation, the translational and rotational motions required for the rearrangement process become increasingly hindered (Scheme 11). Under these conditions, competing paths, such as coupling

Table 8. Product Distributions upon Photolysis of Benzoin Methyl Ether and  $\alpha$ -Propyldeoxybenzoin within Zeolites<sup>a)</sup>

Medium	Type-I Products		Type-II Products	
	Benzil/Pinacol ether	Rearrangement product	Deoxybenzoin	Cyclobutanol
<b>Benzoin methyl ether</b>				
Benzene	26/67	1.0	1	7
Li-X	3	77	13	8
Na-X	4	72	10	14
K-X	7	48	14	18
Rb-X	5	46	18	22
Cs-X	8	34	17	31
<b><math>\alpha</math>-Propyldeoxybenzoin</b>				
Benzene	5/24	—	54	17
Li-X	—	95	4	1
Na-X	—	88	5	7
K-X	—	48	31	21
Rb-X	—	32	22	45
Cs-X	—	21	27	42

<sup>a)</sup> See Scheme 10 for structure of products.

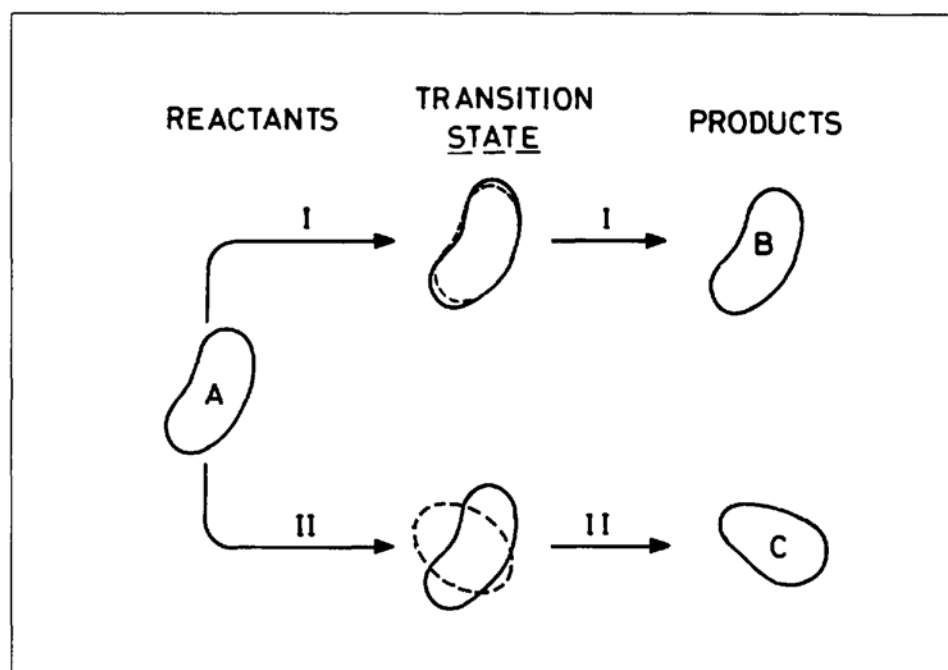


Fig. 21. The reaction cavity of a favorable (I) and unfavorable reaction (II) in an organized medium. Large shape change in II is resisted by the medium [27].

to yield the starting ketone and decarbonylation, both of which require less motion, dominate.

Results presented above clearly illustrate, how one can control the selectivity obtained in a reaction by controlling the size of the reaction cavity.

#### 4.3. Cation Template Effect

Cations present within the supercages of zeolites can be utilized to hold a guest molecule in a particular conformation. The equilibrium distribution of conformers in

a number of carbonyl compounds is influenced by cations, especially by smaller ones such as Li<sup>+</sup> and Na<sup>+</sup>. This is illustrated by comparing the photobehavior of  $\alpha$ -alkyl benzoin ethers and  $\alpha$ -alkyl deoxybenzoins included within cation-exchanged X zeolites (Table 8). The zeolite cavity induces  $\alpha$ -alkyl benzoin ethers to yield products derived *via* the type-II pathway, a minor pathway in benzene. On the other hand, zeolites inhibit  $\alpha$ -alkyl deoxybenzoins from proceeding *via* the type-II pathway, which is favored in benzene. This is

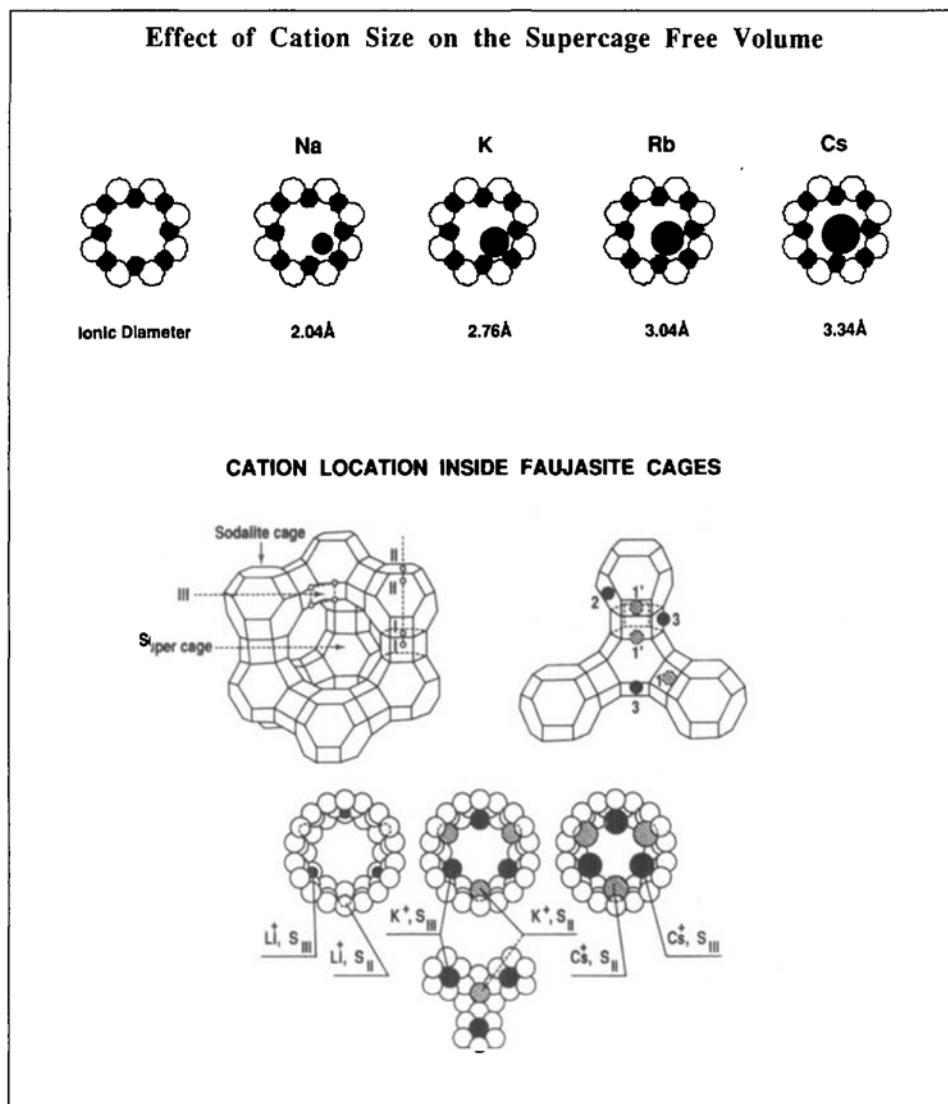


Fig. 22. Illustration of the narrowing of the pore opening of zeolite A resulting from ion-exchange (above). Reduction in available space (relative) within the supercage as the cation size increases (below).

attributed to the ability of the cation present in the cavity to control the conformation of the included molecules (Scheme 12). The presence of an alkoxy chain in  $\alpha$ -alkyl benzoin ethers most likely directs the chelation of the cation to a conformer that is favorable for the type-II process. Similarly, in  $\alpha$ -alkyl deoxybenzoin, the Ph ring directs the conformational preference in the cavity. Such a hypothesis is supported by the results on dealuminated zeolite-Y, in which the Si/Al ratio is very high (>550). At very low levels of Al, the cation concentration is also low. Therefore, conformational control is expected to be minimal and, indeed, only the type-I products dominate the product mixture in both the cases.

### 5. Final Remarks

The approaches taken thus far in 'photochemistry in organized media' can be considered under two categories: one in which the photochemical and photophysical tools are utilized to understand the media itself, and in the second, the media is utilized to modify the photochemical and photophysical behavior of the included guest molecule. In using photochemistry as a tool, fairly well understood and generally well established probes are utilized. There is a tremendous need to understand the physical and chemical characteristics of the internal pore structure of zeolites. In the past, use of photochemistry in this area has not been significant. How-

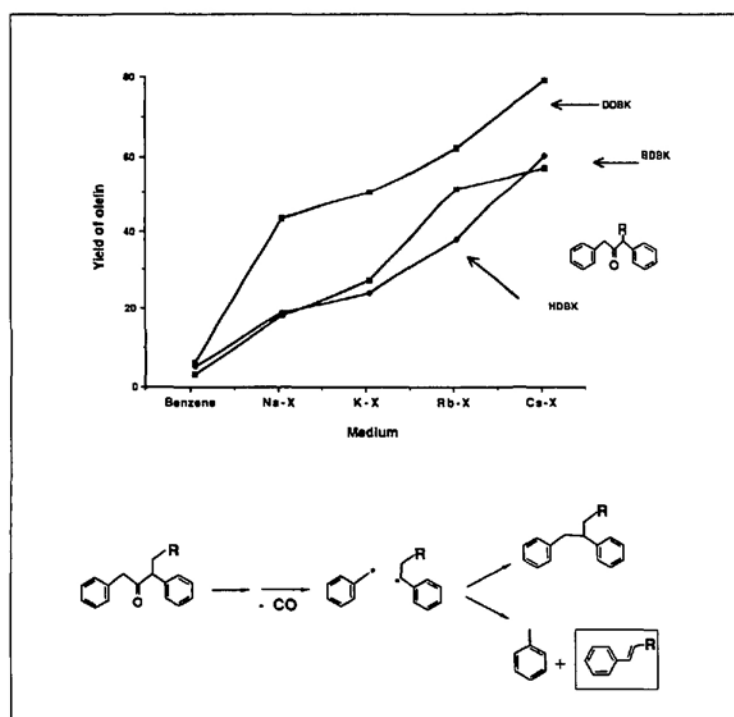


Fig. 23. Dependence of the yield of olefin (disproportionation product) on the cation in the case of  $\alpha$ -alkyl dibenzyl ketones [2c]

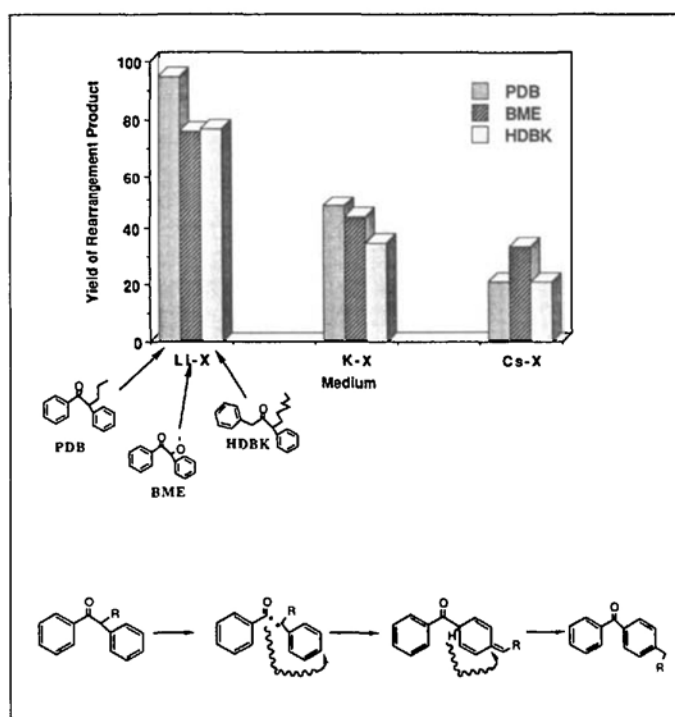
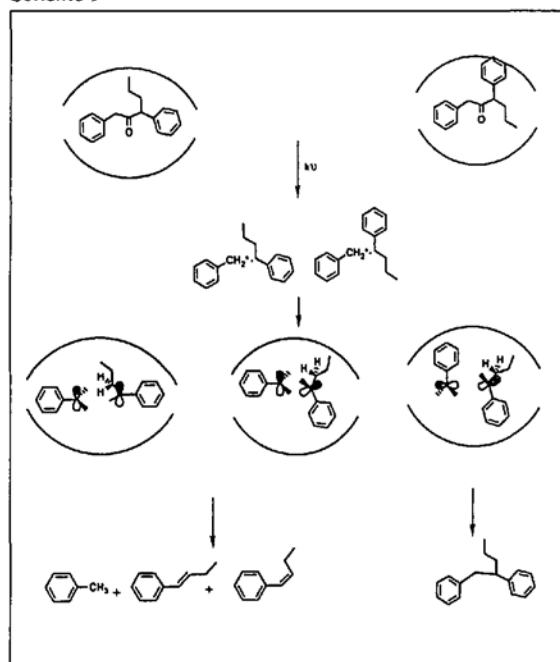


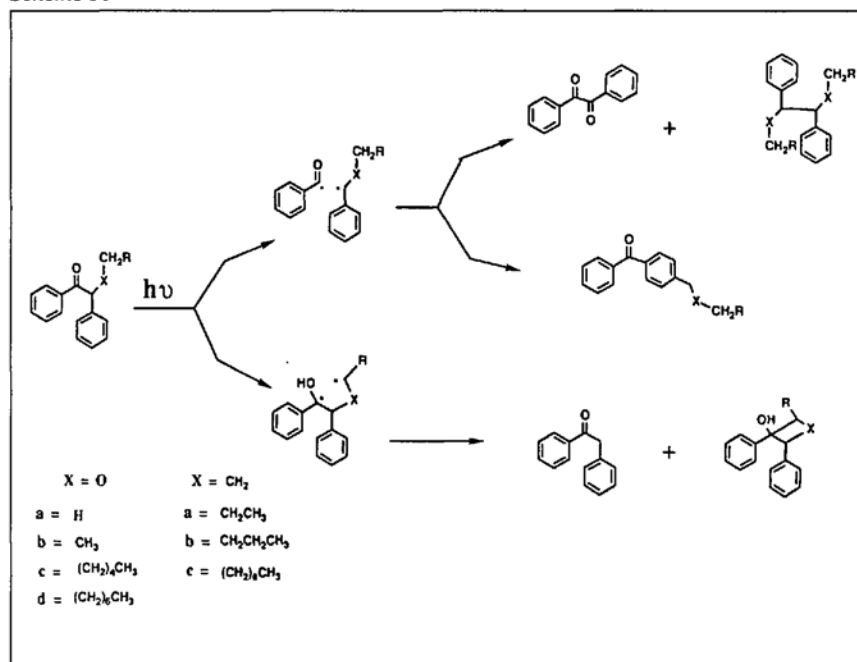
Fig. 24. Dependence of rearrangement process on cations: as the cation size increases the yield of the rearrangement product decreases [2c]



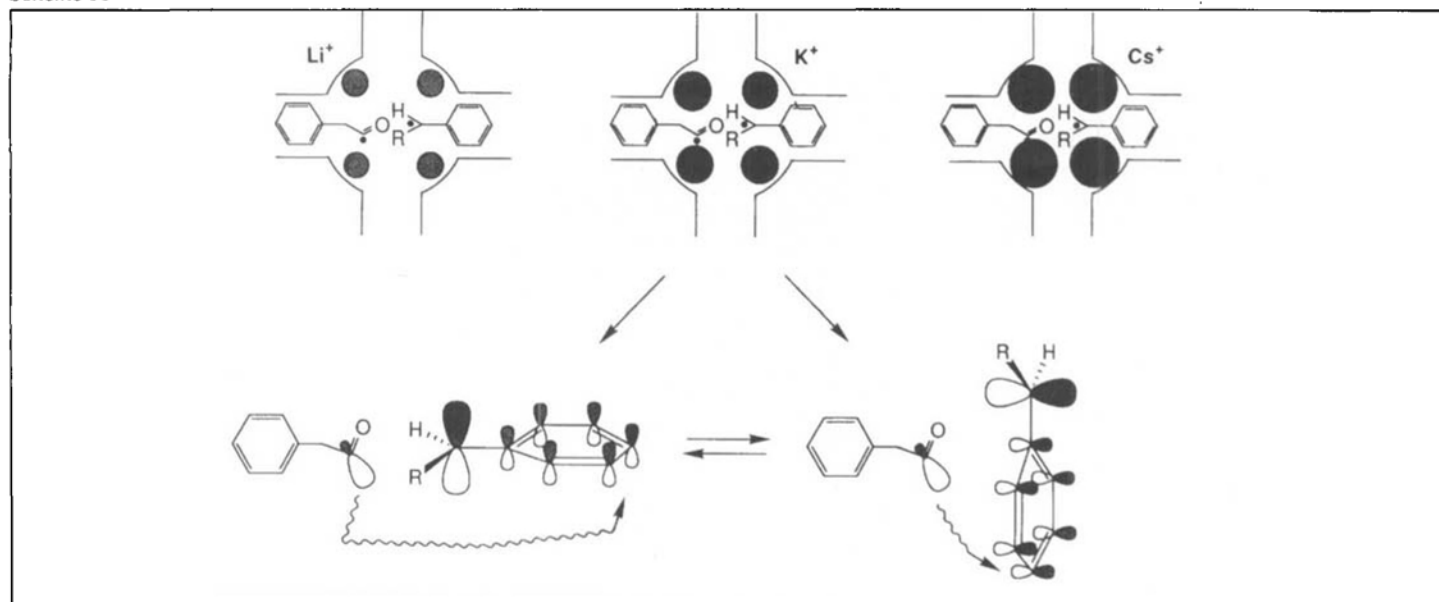
Scheme 9



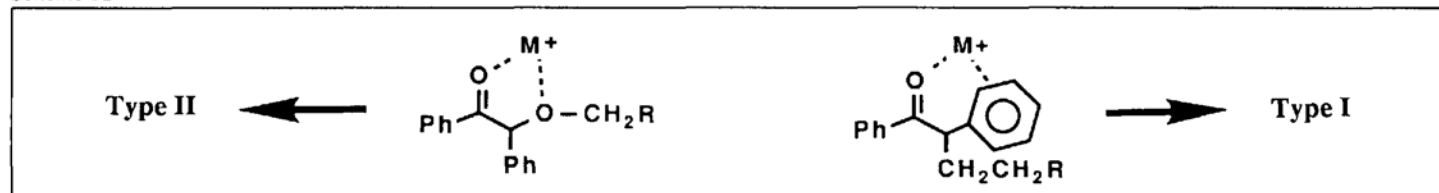
Scheme 10



Scheme 11



Scheme 12



ever, one might predict that in the coming years photochemistry will play a significant role as a tool to understand the physical characteristics of zeolites – location, aggregation, mobility and diffusion of guests within zeolites. Competing techniques such as solid state NMR, laser Raman, X-ray- and neutron-diffraction etc., are more complicated, time consuming and less routine.

Attempts to modify the photochemical and photophysical behavior of a guest

molecule have involved several strategies. In one of them, the rotational and translational motions of a molecule are restricted utilizing a constrained medium. A comparison of the extent of restriction offered by silica and alumina surfaces, clays, and zeolites clearly suggest that zeolites will play an increasingly important role in the future as a medium for a reaction.

The work presented here is the result of an excellent scientific collaboration with Drs. D.R. Corbin, J.V. Caspar, and D.F. Eaton. Outstanding technical assistance provided by D. Sanderson is gratefully acknowledged. Discussions with Profs. N.J. Turro, G.S. Hammond, R.G. Weiss, R.S.H. Liu, and J. Scheffer over a period of time have been very valuable. I take this occasion to thank my other collaborators Profs. C. Dybowski, A. Maki, J. Scheffer, C.V. Kumar, and Dr. L. Johnston whose contributions have been vital to the programme. Special thanks are due to D.F. Eaton who, upon last minute request, delivered the lecture on my behalf.

Received: October 30, 1992

- [1] K. Kalyanasundaram, 'Photochemistry in Microheterogeneous Systems', Academic Press, New York, 1987; T. Matsuura, M. Anpo, Eds., 'Photochemistry on Solid Surfaces', Elsevier, Amsterdam, 1989; V. Ramamurthy, Ed., 'Photochemistry in Organized and Constrained Media', VCH, New York, 1991.
- [2] a) For a summary see: N. J. Turro, *Pure Appl. Chem.* **1986**, *58*, 1219; b) N.J. Turro, in 'Molecular Dynamics in Restricted Geometries', Eds. J. Klafter and J.M. Drake, John Wiley, New York, 1989, p. 387; c) V. Ramamurthy, in 'Photochemistry in Organized and Constrained Media', Ed. V. Ramamurthy, VCH, New York, 1991, p. 429; d) N.J. Turro, M. Garcia-Garibay, in 'Photochemistry in Organized and Constrained Media', Ed. V. Ramamurthy, VCH, New York, 1991, p. 1; e) V. Ramamurthy, D.F. Eaton, J.V. Caspar, *Acc. Chem. Res.* **1992**, *25*, 299.
- [3] D.W. Breck, 'Zeolite Molecular Sieves: Structure, Chemistry, and Use', John Wiley & Sons, New York, 1974; A. Dyer, 'An Introduction to Zeolite Molecular Sieves', John Wiley & Sons, Bath, 1988; H. van Bekkum, E.M. Flanigen, J.C. Jansen, Eds., 'Introduction to Zeolite Science and Practice', Elsevier, Amsterdam, 1991.
- [4] S.P. McGlynn, T. Azumi, M. Kinoshita, 'Molecular Spectroscopy of the Triplet State', Prentice-Hall, Englewood Cliffs, New Jersey, 1969.
- [5] V. Ramamurthy, J.V. Caspar, D.R. Corbin, D.F. Eaton, *J. Photochem. Photobiol. A* **1989**, *50*, 157; J.V. Caspar, V. Ramamurthy, D.R. Corbin, *Coordination Chem. Rev.* **1990**, *97*, 225.
- [6] M. Kasha, *J. Chem. Phys.* **1952**, *20*, 71; D. S. McClure, *ibid.* **1949**, *17*, 905.
- [7] J.M. Larson, L.R. Sousa, *J. Am. Chem. Soc.* **1978**, *100*, 1942; S. Ghosh, M. Petrin, A. H. Maki, L.R. Sousa, *J. Chem. Phys.* **1987**, *87*, 4315; S. Ghosh, M. Petrin, A.H. Maki, L.R. Sousa, *ibid.* **1988**, *88*, 2913.
- [8] V. Ramamurthy, J.V. Caspar, D.R. Corbin, B.D. Schlyer, A.H. Maki, *J. Phys. Chem.* **1990**, *94*, 3391.
- [9] G. Weinzierl, J. Friedrich, *Chem. Phys. Lett.* **1981**, *80*, 55.
- [10] V. Ramamurthy, J.V. Caspar, D.R. Corbin, *Tetrahedron Lett.* **1990**, *31*, 1097.
- [11] J. Saliel, G. E. Khalil, K. Schanze, *Chem. Phys. Lett.* **1980**, *70*, 233; D.F. Evans, *J. Chem. Soc.* **1957**, 1351; R.H. Dyck, D.S. McClure, *J. Chem. Phys.* **1962**, *36*, 2326; H. Gerner, *ibid.* **1989**, *93*, 1826.
- [12] V. Ramamurthy, J.V. Caspar, D.F. Eaton, E.W. Kuo, D.R. Corbin, *J. Am. Chem. Soc.* **1992**, *114*, 3882.
- [13] T.N. Ni, R.A. Caldwell, L.A. Melton, *J. Am. Chem. Soc.* **1989**, *111*, 457; P.M. Crosby, J. M. Dyke, J. Metcalfe, A.J. Rest, K. Salisbury, J.R. Sodeau, *J. Chem. Soc., Perkin Trans. 2* **1977**, 182.
- [14] G. Heinrich, G. Holzer, H. Blume, D. Schulte-Frohlinde, *Z. Naturforsch., B* **1970**, *25*, 496; D.F. Evans, J.N. Tucker, *J. Chem. Soc., Faraday Trans. 2* **1972**, *68*, 174.
- [15] 'Chemistry and physics of matrix isolated species', Eds. L. Andrews and M. Moskovits, North-Holland, Amsterdam, 1989; 'Kinetics and spectroscopy of carbenes and biradicals', Ed. M. Platz, Plenum, New York, 1990; R.F. Childs, G.B. Shaw, *Org. Photochem.* **1991**, *11*, 111; M.S. Platz, E. Leyva, K. Haider, *ibid.* **1991**, *11*, 367; R.S. Sheridan, *ibid.* **1987**, *8*, 159.
- [16] V. Ramamurthy, J.V. Caspar, D.R. Corbin, *J. Am. Chem. Soc.* **1991**, *113*, 594.
- [17] T. Shida, W.H. Hamill, *J. Phys. Chem.* **1966**, *44*, 4372; T. Shida, W.H. Hamill, *ibid.* **1966**, *44*, 2375; Y. Yamamoto, T. Aoyama, K. Hayashi, *J. Chem. Soc., Faraday Trans. 1* **1988**, *84*, 2209.
- [18] Radical ion generation upon photolysis/radiolysis of X or Y zeolite-organic complexes has been reported: K.K. Iu, J.K. Thomas, *J. Phys. Chem.* **1991**, *95*, 506; S. Gosh, N.L. Bauld, *J. Catal.* **1985**, *95*, 300; X.Z. Quin, A.D. Trifunac, *J. Phys. Chem.* **1990**, *94*, 4751; radical ion generation from aromatics upon inclusion in X and Y zeolites has been reported: P.H. Kasi, R.J. Bishop, *ibid.* **1973**, *77*, 2308; D.N. Stammers, J. Turjevich, *J. Am. Chem. Soc.* **1964**, *86*, 749.
- [19] J.V. Caspar, V. Ramamurthy, D.R. Corbin, *J. Am. Chem. Soc.* **1991**, *113*, 600.
- [20] J.C. Scaiano, C. Evans, J.T. Arnason, *J. Photochem. Photobiol. B* **1989**, *3*, 411; C. Evans, J.C. Scaiano, *J. Am. Chem. Soc.* **1990**, *112*, 2694.
- [21] T. A. Skotheim, 'Handbook of Conducting Polymers', Marcel Dekker, Inc., New York, 1986, Vols. 1 and 2; D. Fichou, G. Horowitz, B. Xu, F. Garnier, 'Springer Series in Solid-State Sciences', **1989**, *91*, 386.
- [22] A.O. Patil, A.J. Heeger, F. Wudl, *Chem. Rev.* **1988**, *88*, 183; J.L. Brédas, G.B. Street, *Acc. Chem. Res.* **1985**, *18*, 309; R.H. Baughman, J.L. Bredas, R.R. Chance, R.L. Elsenbaumer, L.W. Shacklette, *Chem. Rev.* **1982**, *82*, 209.
- [23] P. Bauerle, *Adv. Mater.* **1992**, *4*, 102; D. Delabouglise, M. Hmyene, G. Horowitz, A. Yassar, F. Garnier, *ibid.* **1992**, *4*, 102, 107.
- [24] V. Ramamurthy, J.V. Caspar, unpublished results.
- [25] P.M. Lahti, J. Obrzut, F.E. Karasz, *Macromolecules* **1987**, *20*, 2023; T.C. Chung, F. Moraes, J. D. Flood, A. Heeger, *Phys. Rev. B* **1984**, *29*, 2341.
- [26] T. Bally, K. Roth, W. Tang, R.R. Schrock, K. Knoll, L.Y. Park, *J. Am. Chem. Soc.* **1992**, *114*, 2440.
- [27] M.D. Cohen, *Angew. Chem. Int. Ed.* **1975**, *14*, 386; V. Ramamurthy, R.G. Weiss, G.S. Hammond, *Adv. Photochem.*, in press.
- [28] V. Ramamurthy, K. Venkatesan, *Chem. Rev.* **1987**, *87*, 433; K. Venkatesan, V. Ramamurthy, in 'Photochemistry in Organized and Constrained Media', Ed. V. Ramamurthy, VCH, New York, 1991, p. 133; J. R. Scheffer, P. R. Pokkuluri, in 'Photochemistry in Organized and Constrained Media', Ed. V. Ramamurthy, VCH, New York, 1991, p. 185; J.R. Scheffer, M. Garcia-Garibay, O. Nalamatsu, *Org. Photochem.* **1987**, *8*, 249.
- [29] P. J. Wagner, *Acc. Chem. Res.* **1971**, *4*, 168; P.J. Wagner, *ibid.* **1983**, *16*, 461; N.J. Turro, J.C. Dalton, K. Dawes, G. Farrington, R. Hautala, D. Morton, M. Niemczyk, N. Schore, *ibid.* **1971**, *5*, 92; J.C. Scaiano, *ibid.* **1982**, *15*, 252; P. Wagner, B.S. Park, *Org. Photochem.* **1991**, *11*, 227.
- [30] V. Ramamurthy, D.R. Corbin, D.F. Eaton, *J. Chem. Soc., Chem. Commun.* **1989**, 1213; V. Ramamurthy, D.R. Corbin, L.J. Johnston, *J. Am. Chem. Soc.* **1992**, *114*, 3870.
- [31] V. Ramamurthy, D.R. Sanderson, *Tetrahedron Lett.* **1992**, *33*, 2757.
- [32] V. Ramamurthy, J.V. Caspar, D.R. Corbin, D.F. Eaton, J.S. Kaufman, C. Dybowski, *J. Photochem. Photobiol. A* **1990**, *51*, 259.
- [33] V. Ramamurthy, D.R. Corbin, D.F. Eaton, N.J. Turro, *Tetrahedron Lett.* **1989**, *30*, 5833.
- [34] D.R. Corbin, D.F. Eaton, V. Ramamurthy, *J. Am. Chem. Soc.* **1988**, *110*, 4848; D.R. Corbin, D.F. Eaton, V. Ramamurthy, *J. Org. Chem.* **1988**, *53*, 5384; V. Ramamurthy, D.R. Corbin, D.F. Eaton, *ibid.* **1990**, *55*, 5269.